13

Calculation of Momentum Space Integrals

In the last chapter we have shown that the problem of determining the counterterms in ϕ^4-theory can be reduced completely to the calculation of massless Feynman integrals in momentum space. Among these, the massless propagator-type integrals generated by the technique of infrared rearrangement in Section 12.2 can be calculated most easily by algebraic methods. The result of a successive application of a generic one-loop integral formula in momentum space yields a Laurent expansion in ε. Some of the integrals can be solved rather directly, others can only be reduced to certain generic two-, three- or four-loop integrals. These can be evaluated by a reduction algorithm in momentum space [1] explained in Section 13.4. In this way, we can find all integrals up to four loops, and most of the five-loop integrals. Some of the five-loop diagrams contain one special type of integrals and a few individual integrals, for which the above reduction algorithm fails. These integrals were initially determined numerically in configuration space, by applying the so-called Gegenbauer-polynomial-**x**-space technique (GPXT) [2]. Later, however, analytic solutions were found by the method of ideal index constellations [3] described in Section 13.5. With these methods, the pole terms of all Feynman integrals up to five loops have been found analytically. In this chapter we shall be concerned only with the momentum integrals associated with the Feynman diagrams. For this reason, we shall ignore the coupling constants attached to the vertices of the diagrams in the Feynman rule (3.5) of the perturbation expansion.

13.1 Simple Loop Integrals

The calculation of all Feynman integrals in momentum space proceeds from the simplest massless loop integral

$$\int \frac{d^Dp}{(2\pi)^D}\,\frac{1}{(\mathbf{p}^2)^a[(\mathbf{p}-\mathbf{k})^2]^b} \;=\; \mathbf{k}\;\overset{a}{\underset{b}{\bigcirc}}\; . \tag{13.1}$$

For $\mathbf{k}=0$, this integral vanishes by Veltman's formula (8.33). The powers a and b of the massless propagators will be called *line indices*. Initially, the line indices of the simple loop diagram are both equal to unity. However, differentiations with respect to the mass or the external momenta discussed in the last chapter, or successive calculations of nested simple loops, will generate indices greater than one. Working in dimensions $D=4-\varepsilon$, the line indices will in general be noninteger, but always close to integer with a typical noninteger form $a=p+q\varepsilon/2$, where p and q are integer.

The D-dimensional Fourier representation of a massless propagator with line index a is, as shown in detail in Appendix 13A,

$$\frac{1}{(\mathbf{p}^2)^a} \;=\; \frac{1}{\pi^{D/2}\,4^a}\frac{\Gamma(D/2-a)}{\Gamma(a)}\int d^Dx\,\frac{e^{i\mathbf{p}\mathbf{x}}}{(\mathbf{x}^2)^{D/2-a}}\;. \tag{13.2}$$

We shall also define a line index in configuration space as the power of $1/\mathbf{x}^2$ in a massless integral. In the Fourier integral (13.2), this line index is $a' = D/2 - a$. Inserting (13.2) into (13.1), we find the Fourier representation of the simple loop integral:

$$= \int \frac{d^Dp}{(2\pi)^D} \frac{1}{(\mathbf{p}^2)^a[(\mathbf{p}-\mathbf{k})^2]^b}$$

$$= \frac{\Gamma(D/2-a)\Gamma(D/2-b)}{\pi^D\Gamma(a)\Gamma(b)4^{a+b}} \int \frac{d^Dp}{(2\pi)^D} \int d^Dx\, d^Dy\, \frac{\mathrm{e}^{i[\mathbf{px}+(\mathbf{k}-\mathbf{p})\mathbf{y}]}}{(\mathbf{x}^2)^{D/2-a}(\mathbf{y}^2)^{D/2-b}}\,. \tag{13.3}$$

The momentum integral gives rise to a $\delta^{(D)}$-function, forcing $\mathbf{y}$ to be equal to $\mathbf{x}$, so that we obtain

$$= \frac{\Gamma(D/2-a)\Gamma(D/2-b)}{\pi^D\Gamma(a)\Gamma(b)4^{a+b}} \int d^Dx\, \frac{\mathrm{e}^{i\mathbf{kx}}}{(\mathbf{x}^2)^{D-a-b}}. \tag{13.4}$$

The integral of the right-hand side will be represented graphically by a line marked by its $\mathbf{x}$-space index, leading to the graphical correspondence

$$\propto$$

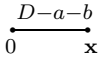

.

Using once more Formula (13.2), the $\mathbf{x}$-space integral on the right-hand side can be evaluated, and we obtain

$$= \frac{\Gamma(D/2-a)\,\Gamma(D/2-b)}{\pi^D\,\Gamma(a)\,\Gamma(b)\,4^{(a+b)}} \int d^Dx\, \frac{e^{i\mathbf{kx}}}{(\mathbf{x}^2)^{D/2-(a+b-D/2)}}$$

$$= \frac{\Gamma(D/2-a)\Gamma(D/2-b)\Gamma(a+b-D/2)}{(4\pi)^{D/2}\,\Gamma(a)\Gamma(b)\Gamma(D-a-b)} \frac{1}{(\mathbf{k}^2)^{a+b-D/2}}$$

$$= \frac{1}{(\mathbf{k}^2)^{a+b-D/2}}\; \frac{1}{(4\pi)^2} L(a,b)\;. \tag{13.5}$$

The quantity $L(a,b)$ will be referred to as the *loop function*. Its prefactor $1/(4\pi)^2$ will later be absorbed into the coupling constant (see Subsection 13.1.2). In terms of the Beta function $B(x,y) = \Gamma(x)\Gamma(y)/\Gamma(x+y)$, and the function

$$\nu(x) \equiv \Gamma(D/2-x)/\Gamma(x), \tag{13.6}$$

the loop function can be rewritten conveniently as

$$L(a,b) = (4\pi)^{\varepsilon/2}\; B(D/2-a, D/2-b)\; \frac{\Gamma(a+b-D/2)}{\Gamma(a)\Gamma(b)}$$

$$= (4\pi)^{\varepsilon/2}\, \nu(a)\, \nu(b)\, \nu(D-a-b)\;. \tag{13.7}$$

Differentiation of a propagator with respect to the momentum generates lines with vector indices of the type introduced in Sections 11.8 and 12.2.2:

$$\frac{\partial}{\partial p_\mu} \frac{1}{(\mathbf{p}^2)^{a-1}} = -\,2(a-1)\, \frac{p_\mu}{(\mathbf{p}^2)^a}\;. \tag{13.8}$$

Using (13.2), we obtain the Fourier representation

$$\begin{aligned}\frac{p_\mu}{(\mathbf{p}^2)^a} &= \frac{-1/2}{(a-1)}\frac{\partial}{\partial p_\mu}\frac{1}{(\mathbf{p}^2)^{a-1}} \\ &= \frac{-1/2\,\Gamma(D/2-a+1)}{\pi^{D/2}4^{a-1}\Gamma(a)}\int d^Dx\,\frac{ix_\mu\,\mathrm{e}^{i\mathbf{p}\cdot\mathbf{x}}}{(\mathbf{x}^2)^{D/2-a+1}}\,. \end{aligned} \tag{13.9}$$

A simple loop integral (13.1) containing a line with a vector index has therefore a Fourier representation

$$\begin{aligned} &= \int\frac{d^Dp}{(2\pi)^D}\frac{p_\mu}{(\mathbf{p}^2)^a[(\mathbf{p}-\mathbf{k})^2]^b} \\ &= -\frac{1}{2}\frac{\Gamma(D/2-a+1)\Gamma(D/2-b)}{\pi^D4^{(a+b-1)}\Gamma(a)\Gamma(b)}\int d^Dx\frac{i\,x_\mu\,\mathrm{e}^{i\mathbf{k}\cdot\mathbf{x}}}{(\mathbf{x}^2)^{D-a-b+1}}\,, \end{aligned} \tag{13.10}$$

where the vertical dash across the upper line of the diagram indicates the vector index [recall Eq. (11.49)]. The right-hand side is evaluated by an inverse Fourier transformation as

$$= \frac{\Gamma(D/2-a+1)\Gamma(D/2-b)\Gamma(a+b-D/2)}{(4\pi)^{D/2}\;\Gamma(a)\;\Gamma(b)\;\Gamma(D-a-b+1)}\frac{k_\mu}{(\mathbf{k}^2)^{a+b-D/2}}. \tag{13.11}$$

We also introduce the generalized loop function

$$L^{(k)}(a,b) = (4\pi)^{\varepsilon/2}\;B(D/2-a+k,D/2-b)\;\frac{\Gamma(a+b-D/2)}{\Gamma(a)\Gamma(b)}\,, \tag{13.12}$$

of which the original loop function (13.7) is the special case $L^{(0)}(a,b)$. In contrast to $L(a,b) = L^{(0)}(a,b)$, the functions $L^{(k)}(a,b)$ are not symmetric in a and b. In terms of $L^{(k)}(a,b)$, we write the result (13.11) as

$$= \frac{1}{(4\pi)^2}\;L^{(1)}(a,b)\,\frac{k_\mu}{(\mathbf{k}^2)^{a+b-D/2}}\,. \tag{13.13}$$

13.1.1 Expansion of Loop Function

A Laurent expansion of the loop function $L(a,b)$ in (13.7) in powers of ε contains at most a simple pole in ε. This is the only singularity caused by the simple loop integral. In order to find its residue, we rewrite (13.7) more explicitly as

$$L(a,b) = (4\pi)^{\varepsilon/2}\,\frac{\Gamma(D/2-a)\Gamma(D/2-b)\Gamma(a+b-D/2)}{\Gamma(a)\Gamma(b)\Gamma(D-a-b)}\,, \tag{13.14}$$

and expand each Gamma function $\Gamma(n+\alpha\varepsilon)$ as follows:

$$\Gamma(n+z) = (n-1)!\,\exp\Big\{-z\Big[\gamma-\zeta^{(n)}(1)\Big]+\sum_{j=2}^{\infty}(-1)^j\,\frac{z^j}{j}\,\Big[\zeta(j)-\zeta^{(n)}(j)\Big]\Big\}\,. \tag{13.15}$$

This formula is derived in Appendix 13B [see Eq. (13B.12)]. The formula contains Riemann's zeta function

$$\zeta(z) = \sum_{l=1}^{\infty}\frac{1}{l^z}\,, \tag{13.16}$$

and Euler's constant $\gamma = 0.5772\ldots$ [recall (8D.10)]. The symbol $\zeta^{(n)}(z)$ denotes the *truncated zeta function*

$$\zeta^{(n)}(z) = \sum_{l=1}^{n-1} \frac{1}{l^z}, \tag{13.17}$$

with the special values

$$\zeta^{(1)}(j) = 0, \quad \zeta^{(2)}(j) = 1, \quad \zeta^{(n)}(0) = n-1\,. \tag{13.18}$$

Using the expansion (13.15), the Gamma functions in (13.14) may be written as products of exponentials, each expanded in powers of ε. For the simple loop function $L(a,a)$ with $a=b=1$, the expansion reads

$$\begin{aligned} L(1,1) &= (4\pi)^{\varepsilon/2}\frac{\Gamma(D/2-1)\Gamma(D/2-1)\Gamma(2-D/2)}{\Gamma(1)\Gamma(1)\Gamma(D-2)} = (4\pi)^{\varepsilon/2}\frac{[\Gamma(1-\varepsilon/2)]^2\Gamma(1+\varepsilon/2)}{(\varepsilon/2)\,\Gamma(2-\varepsilon)} \\ &= (4\pi)^{\varepsilon/2}\frac{2}{\varepsilon}\,\exp\left[-\frac{\varepsilon}{2}\gamma + \varepsilon\zeta^{(2)}(1)\right] \\ &\quad \times \exp\left\{\sum_{j=2}^{\infty}\frac{[2+(-1)^j)]\,(\varepsilon/2)^j}{j}\left[\zeta(j) - \underbrace{\zeta^{(1)}(j)}_{=0}\right] - \sum_{j=2}^{\infty}\frac{\varepsilon^j}{j}\left[\zeta(j) - \underbrace{\zeta^{(2)}(j)}_{=1}\right]\right\}, \end{aligned}$$

and can be brought to the form

$$L(1,1) = \frac{2}{\varepsilon}\exp\left\{\frac{\varepsilon}{2}\left[\ln 4\pi - \gamma - \frac{\varepsilon}{4}\zeta(2)\right]\right\}\exp\left[\sum_{j=1}^{\infty}\frac{\varepsilon^j}{j} + \sum_{j=3}^{\infty}\frac{2+(-1)^j-2^j}{2^j}\zeta(j)\frac{\varepsilon^j}{j}\right] \equiv \frac{2}{\varepsilon}\,L_0(\varepsilon). \tag{13.19}$$

On the right-hand side we have factored out a pole term of the form $2/\varepsilon$, defining a finite residue function $L_0(\varepsilon)$ whose Taylor series expansion starts out like $1+\mathcal{O}(\varepsilon)$:

$$L_0(\varepsilon) \equiv \frac{\varepsilon}{2}L(1,1) = 1 + \frac{\varepsilon}{2}\,(\ln 4\pi - \gamma + 2) + \ldots\,. \tag{13.20}$$

Any loop integral $L(a,b)$ can ultimately be reduced to this function $L_0(\varepsilon)$. In a first step, the integer part of the parameters is reduced [4]:

$$L(a,b) = \frac{(a+b-1-D/2)(D-2-a-b)}{(b-1)(D/2-2-b)}L(a,b-1). \tag{13.21}$$

With the help of this formula and the symmetry $L(a,b) = L(b,a)$, the parameters a,b can always be reduced to being near unity up to terms of order ε, say $a = 1+\alpha\varepsilon$ and $b = 1+\beta\varepsilon$. For such parameters, the expansion of the loop-function reads

$$\begin{aligned} L(1+\alpha\varepsilon, 1+\beta\varepsilon) &= \frac{(4\pi)^{\varepsilon/2}}{\varepsilon(\alpha+b+1/2)}\frac{\Gamma(1-(\alpha+\frac{1}{2})\varepsilon)\Gamma(1-(\beta+1/2)\varepsilon)\Gamma(1+(\alpha+\beta+1/2)\varepsilon)}{\Gamma(1+\alpha\varepsilon)\Gamma(1+\beta\varepsilon)\Gamma(2-(\alpha+\beta+1)\varepsilon)} \\ &= \frac{2}{\varepsilon\,(2\alpha+2\beta+1)}\exp\left\{\frac{\varepsilon}{2}\left[\ln 4\pi - \gamma - \frac{\varepsilon}{4}\zeta(2)\right]\right\} \\ &\quad \times \exp\left[\sum_{j=1}^{\infty}(\alpha+\beta+1)^j\frac{\varepsilon^j}{j} + \sum_{j=3}^{\infty}F(\alpha,\beta,j)\zeta(j)\frac{\varepsilon^j}{j}\right], \end{aligned} \tag{13.22}$$

where

$$F(\alpha,\beta,j) = (\alpha+\tfrac{1}{2})^j + (\beta+\tfrac{1}{2})^j + (-\alpha-\beta-\tfrac{1}{2})^j - (-\alpha)^j - (-\beta)^j - (\alpha+\beta+1)^j. \tag{13.23}$$

In actual calculations, the direct expansion in Eq. (13.15) turns out to be most convenient. In order to avoid errors, a computer-algebraic program is extremely useful. We have employed the program REDUCE. The calculations up to six loops in this text require an expansion of the loop function up to the seventh order in ε [7].

13.1.2 Modified MS-Scheme and Various Redefinitions of Mass Scale

There are several factors common to all loop integrals. Such factors can be removed by a redefinition of the coupling constant. The reason for this lies in the fixed relationships between the number of loops L and the number of vertices p in the relevant two- and four-point diagrams. From Eqs. (9.2) and (9.5) we see that $L = p$ for the Feynman integrals of the two-point functions, and $L = p - 1$ for those of the four-point functions. Thus we may always go from g to some modified coupling constant $\bar{g} = g\times\text{constant}\times f(\varepsilon)$ with $f(\varepsilon) = 1 + f_1\varepsilon + f_2\varepsilon^2 + \dots$, and the factor $f(\varepsilon)$ will disappear from the final expansions of the renormalization constants. This observation was made before [recall Eq. (9.75)]. In the above loop calculations in Eq. (13.5), the constant may be chosen to be $1/(4\pi)^2$. This was the reason for expressing all renormalization group functions in powers of

$$\bar{g} = \frac{g}{(4\pi)^2} \tag{13.24}$$

in Eqs. (10.55)–(10.58). This will be done for all higher-loop expansions in Chapter 15.

Although an ε-dependent common factor $f(\varepsilon) = 1+f_1\varepsilon+f_2\varepsilon^2+\dots$ in all loop integrals does not show up in the final expansions, certain ways of choosing them offer different advantages in the calculations. A strict minimal subtraction scheme works with $f(\varepsilon) \equiv 1$, and expands all ε-dependent factors in $L(a, b)$ in powers of ε, as we did with the common factor $f(\varepsilon) = 1/(4\pi)^{-\varepsilon/2}$ in our two-loop calculation in Subsection 9.3.2. Other authors have modified this scheme by keeping some specific nontrivial function $f(\varepsilon)$ unexpanded, and absorbing it into the coupling constant. In fact, if such a function appears as a factor, it may simply be omitted from the calculations by assuming that it has been absorbed into the arbitrary mass scale μ. Such a function $f(\varepsilon)$ constitutes a common portion of all loop functions $L(a, b)$. A so-called $\overline{\text{MS}}$-scheme in the literature omits a factor $(4\pi)^{\varepsilon/2}\exp(-\gamma\varepsilon/2)$. This scheme is favored in quantum chromodynamics (QCD). It permits us to drop all terms 4π and γ in the ε-expansions (13.19) and (13.22). In higher loop-calculations, it is useful to omit also all terms containing $\zeta(2)$ [8]. This amounts to absorbing a function

$$f(\varepsilon) = \exp\left\{\frac{\varepsilon}{2}\left[\ln 4\pi - \gamma - \frac{\varepsilon}{4}\zeta(2)\right]\right\} \tag{13.25}$$

into the mass scale μ. If we remove this factor from the loop integral (13.19), it goes over into the new loop function

$$L(1,1)_{\text{ours}} \equiv L(1,1)_{\overline{\text{MS}}} = \frac{2}{\varepsilon}\exp\left\{\sum_{j=1}^{\infty}\frac{\varepsilon^j}{j} + \sum_{j=3}^{\infty}\left[\frac{2+(-1)^j-2^j}{j}\left(\frac{\varepsilon}{2}\right)^j\zeta(j)\right]\right\}, \tag{13.26}$$

which we shall use in all our calculations. We shall also refer to our scheme as an $\overline{\text{MS}}$-scheme, even if it is, strictly speaking, an extended version of the standard $\overline{\text{MS}}$-scheme. Thus we shall denote it by $L(1,1)_{\overline{\text{MS}}}$. Its first terms in an ε-expansion are

$$L(1,1)_{\overline{\text{MS}}} = \frac{2}{\varepsilon} + 2 + 2\,\varepsilon - \varepsilon^2\left[\frac{7}{12}\zeta(3) - 2\right] - \varepsilon^3\left[\frac{13}{32}\zeta(4) + \frac{7}{12}\zeta(3) - 2\right] + \mathcal{O}(\varepsilon^4)\,. \tag{13.27}$$

Usually, we shall omit the subscript for notational convenience without much danger of confusion. The loop function $L(1,1)_{\overline{\rm MS}}$ can always be distinguished from the original in (13.19) by the absence of all terms containing ln 4π, γ, and $\zeta(2)$.

13.1.3 Further Subtraction Schemes

Let us briefly indicate the characteristic features of other subtraction schemes.

a) The *L-scheme* [5] uses the fact that each loop function $L(a,b)$ can be reduced algebraically to $L(1,1) = 2L_0(\varepsilon)/\varepsilon$ as shown in Subsection 13.1.1. The expansion coefficients contain the ζ-function only with arguments $n > 2$:

$$L(a,b) = L(1,1) \sum_{n=0}^{\infty} C_n(a,b,\zeta(j>2))\,\varepsilon^n = L_0\,\frac{2}{\varepsilon} \sum_{n=0}^{\infty} C_n(a,b,\zeta(j>2))\,\varepsilon^n\,. \tag{13.28}$$

This scheme absorbs the complete function $L_0(\varepsilon) = f(\varepsilon)$ into the mass scale μ. An important advantage of this scheme is that the Gamma functions require no longer an expansion in powers of ε. There is, however, a disadvantage to this scheme: all loop functions $L(a,b)$ must be re-expressed explicitly in terms of $L(1,1)$.

b) The $\mathcal{S}_D$-scheme [6] uses the fact that every loop integration involves the surface of the D-dimensional unit sphere $S_D = 2\pi^{D/2}/\Gamma(D/2)$ and a factor $1/(2\pi)^D$. By analogy with $\hbar \equiv h/2\pi$ we define $\mathcal{S}_D \equiv S_D/(2\pi)^D$, and a new coupling constant

$$\begin{aligned} g_{\mathcal{S}_D} &= \mathcal{S}_D\, g = \frac{2}{(4\pi)^{D/2}\Gamma(D/2)}\, g \\ &= \frac{2}{(4\pi)^{2-\varepsilon/2}} \exp\left\{\frac{\varepsilon}{2} - \sum_{j=1}^{\infty} \frac{(\varepsilon/2)^j}{j}\,[\zeta(j)-1]\right\} g. \end{aligned} \tag{13.29}$$

There appears then a factor 2 which shows up in all expansions. The accompanying function of ε

$$f(\varepsilon) = \frac{1}{(4\pi)^{-\varepsilon/2}} \exp\left\{\frac{\varepsilon}{2} - \sum_{j=1}^{\infty} \frac{(\varepsilon/2)^j}{j}\,[\zeta(j)-1]\right\} \tag{13.30}$$

can again be dropped by absorbing it into the arbitrary mass scale μ. Using $g_{\mathcal{S}_D}$, the effective loop function which remains after factorizing out the ε-expansion for $\mathcal{S}_D$ in (13.26) is

$$\begin{aligned} L(1,1)_{\mathcal{S}_D} &= \frac{1}{\varepsilon}\,\exp\left\{\sum_{j=3}^{\infty}\left[\frac{3+(-1)^j-2^j}{j}\left(\frac{\varepsilon}{2}\right)^j\zeta(j)\right] + \sum_{j=1}^{\infty}\left[\frac{\varepsilon^j}{j} - \frac{(\varepsilon/2)^j}{j}\right]\right\} \\ &= \frac{1}{\varepsilon} + \frac{1}{2} + \frac{1}{2}\,\varepsilon + \varepsilon^2\left[\frac{1}{2} - \frac{1}{4}\zeta(3)\right] + \varepsilon^3\left[\frac{1}{12} - \frac{1}{8}\zeta(3) - \frac{3}{16}\zeta(4)\right] + \mathcal{O}(\varepsilon^4)\,. \end{aligned}$$

As in our $\overline{\rm MS}$-scheme, the sum over j does not contain any constants ln 4π, γ, and $\zeta(2)$, but the remaining expansion is quite different from that in Eq. (13.27).

13.2 Classification of Diagrams

The set of all loop diagrams can be subdivided into three classes:

a) Diagrams with cutvertices, which factorize into independent integrals of lower-order diagrams.

For example:

$$= \int \frac{d^Dp}{(2\pi)^D} \frac{1}{\mathbf{p}^2(\mathbf{p}-\mathbf{k})^2} \int \frac{d^Dq}{(2\pi)^D} \frac{1}{\mathbf{q}^2(\mathbf{q}-\mathbf{k})^2}$$

$$= \left[\frac{1}{(4\pi)^2}\right]^2 L(1,1)\, L(1,1) \frac{1}{(\mathbf{k}^2)^{4-D}} \,.$$

b) *Primitive diagrams*, which consist of nested simple loops and can be calculated recursively.

The integration of a simple loop with line indices a and b raises the line index of its external momentum by $a+b-D/2$, i.e. for $a=1,\ b=1$ by $2-D/2=\varepsilon/2$. Each integration produces a loop function $L(a,b)$, so that a diagram with L loops generates at most a pole of Lth order in ε. For example:

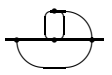

$$= \int \frac{d^Dp}{(2\pi)^D} \frac{d^Dq}{(2\pi)^D} \frac{d^Dr}{(2\pi)^D} \frac{1}{\mathbf{p}^2(\mathbf{p}-\mathbf{r})^2\mathbf{r}^2(\mathbf{r}-\mathbf{q})^2\mathbf{q}^2(\mathbf{q}-\mathbf{k})^2}$$

$$= \left[\frac{1}{(4\pi)^2}\right]^3 L(1,1)\, L(1,1+\varepsilon/2)\, L(1,1+\varepsilon) \frac{1}{(\mathbf{k}^2)^{\frac{3}{2}\varepsilon}} \,.$$

c) *Generic ϕ^3-diagrams*, which do not belong to the above two classes.

All ϕ^4- and ϕ^3-diagrams may be generated by shrinking lines and choosing appropriate line indices in a generic diagram with the same number of loops. The generic two- and three-loop diagrams are shown in Fig. 13.1. According to their shape, they are called KITE, BENZ, LADDER, and NONPLANAR types.

KITE BENZ LADDER NONPLANAR

FIGURE 13.1 Generic two- and three-loop diagrams. Only one generic two-loop diagram occurs, and three with three loops. The numbers label the line indices.

It can be shown [1] that the calculation of all propagator-type integrals up to three loops can ultimately be reduced to the evaluation of one of the generic diagrams in Fig. 13.1, or a primitive diagram. The technique of IR-rearrangement transforms most of the ϕ^4-diagrams up to five loops either into generic two- or three-loop diagrams with insertions of simple loops in their lines, or into simple loops with generic two- or three-loop subdiagrams. The more difficult ones will still contain generic four-loop diagrams, and in one case even a generic five-loop diagram. The five-loop diagrams, to be shown in Fig. 13.10, will pose the main problems in the calculation. Algorithms for the reduction to simple loops exist only for the generic two- and three-loop diagrams, and not even for these with all line index constellations. Those diagrams have to be avoided by IR-rearrangement whenever possible.

13.3 Five-Loop Diagrams

Whenever possible, the five-loop diagrams are IR-rearranged in order to form a simple loop with one or more insertions. The resulting propagator-type integrals may then have ϕ^3- or

ϕ^5-vertices. The lower loop insertions must, unfortunately, be calculated up to the finite terms of order $\mathcal{O}(\varepsilon^0)$ because the associated simple loop integral will make it appear in a pole term in ε.

Some examples are drawn in Fig. 13.2 to illustrate the occurrence of the generic ϕ^3-diagrams in the IR-rearranged five-loop ϕ^4-diagrams. The Feynman integrals of the generic types are functions of the line indices, for which we shall use the notation $\mathrm{KI}(a_1,\ldots,a_5)$, $\mathrm{BE}(a_1,\ldots,a_8)$, $\mathrm{LA}(a_1,\ldots,a_8)$, $\mathrm{NO}(a_1,\ldots,a_8)$ for the KITE, BENZ, LADDER, and NONPLANAR types, respectively. The first five examples drawn below are typical of what may be encountered in many five-loop diagrams, generic two- and three-loop diagrams with shrunk lines or combined with simple loops. Full generic three-loop diagrams with no shrunk line appear quite rarely, and each only once. These are of the BENZ type (No. 34), the LADDER type (No. 25), and the NONPLANAR type (No. 28), where the numbers are the running numbers of the diagrams used in Appendix A.

No. 102 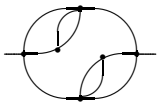

consists entirely of nested simple loops and is given by $L(1,1)L(1,1+\varepsilon/2)L(1,1)L(1,1+\varepsilon/2)L(1+\varepsilon,1+\varepsilon)$.

No. 55 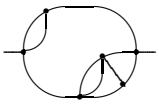

requires $\mathrm{KI}(\varepsilon/2,1,1,1,1)$ up to $\mathcal{O}(\varepsilon^2)$: $\mathrm{KI}(\varepsilon/2,1,1,1,1)L(1+\varepsilon/2,1+3\varepsilon/2)[L(1,1)]^2$.

No. 107 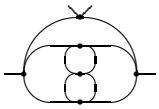

requires the KITE type, $\mathrm{KI}(1,1,1,1,\varepsilon)$, up to $\mathcal{O}(\varepsilon^2)$: $\mathrm{KI}(1,1,1,1,\varepsilon)L(1,1+2\varepsilon)[L(1,1)]^2$.

No. 111 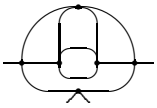

requires the BE integral with $\varepsilon/2$ on line 2 and line 8 shrunk, $\mathrm{BE}(1,\varepsilon/2,1,1,1,1,1,0)$, up to $\mathcal{O}(\varepsilon^1)$: $\mathrm{BE}(1,\varepsilon/2,1,1,1,1,1,0)L(1,1+2\varepsilon)L(1,1)$.

No. 25 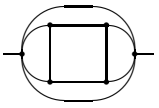

requires $\mathrm{LA}(1,1,1,1,1,1,1,1)$ up to $\mathcal{O}(\varepsilon)$. Note that this term is IR-divergent: $\mathrm{LA}(1,1,1,1,1,1,1,1)L(1,2+3\varepsilon/2)L(1,1+2\varepsilon)$.

No. 3 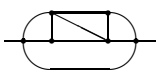

includes a generic four-loop diagram. It is one of the six diagrams in Fig. 13.10 requiring special methods. It has to be multiplied by $L(1,1+2\varepsilon)$.

FIGURE 13.2 Examples of occurrence of the generic ϕ^3-diagrams in IR-rearranged five-loop ϕ^4-diagrams.

13.4 Reduction Algorithm based on Partial Integration

A method based on *partial integration* provides us with an algorithm for the reduction of generic two- and three-loop diagrams to primitive diagrams, which can then be calculated to all orders in ε [1]. As announced at the beginning of this chapter, this will enable us to calculate all diagrams of the KITE, BENZ, and LADDER type, if certain line indices are integers. For diagrams with noninteger indices we shall have to resort to the configuration-space methods to be described in Subsection 13.5. Diagrams with simple loop insertions on such a line will have a noninteger line index and therefore cannot be reduced by the algorithm.

The typical loop integral which becomes accessible via the method of partial integration is the triangle diagram in Fig. 13.3. It appears as a subdiagram in all generic diagrams in Fig. 13.1. The associated integrand has the form $1/(\mathbf{p}^2)^a[(\mathbf{p}-\mathbf{q})^2]^b[(\mathbf{p}-\mathbf{k})^2]^c$, and this type of integrals can be reduced to simple loop integrals by partial integration.

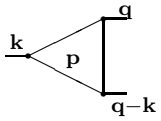

FIGURE 13.3 The triangle-subdiagram which appears in the KITE, LADDER, and BENZ type.

13.4.1 Triangle Diagram

Since surface terms vanish in dimensional regularization, partial integrations are a useful tool in the evaluation of massless Feynman integrals. They lead directly to a reduction algorithm for the integration of the triangle in Fig. 13.3. For this we insert into the integral the identity

$$D \equiv \partial/\partial p_\mu (p-q)_\mu, \tag{13.31}$$

where D is the dimension of space, and perform an integration by parts

$$\begin{aligned} D\int \frac{d^Dp}{(2\pi)^D}\frac{1}{\mathbf{p}^2(\mathbf{p}-\mathbf{q})^2(\mathbf{p}-\mathbf{k})^2} &= \int \frac{d^Dp}{(2\pi)^D}\left[\frac{\partial}{\partial p_\mu}(p-q)_\mu\right]\frac{1}{\mathbf{p}^2(\mathbf{p}-\mathbf{q})^2(\mathbf{p}-\mathbf{k})^2} \\ &= -\int \frac{d^Dp}{(2\pi)^D}\,(p-q)_\mu\,\frac{\partial}{\partial p_\mu}\frac{1}{\mathbf{p}^2(\mathbf{p}-\mathbf{q})^2(\mathbf{p}-\mathbf{k})^2}. \end{aligned} \tag{13.32}$$

We may demonstrate explicitly the vanishing of the neglected surface term in dimensional regularization by considering its Fourier representation, obtained with the help of Eqs. (13.2) and (13.9) for $a=1$:

$$\int \frac{d^Dp}{(2\pi)^D}\frac{\partial}{\partial p_\mu}\frac{(p-q)_\mu}{\mathbf{p}^2(\mathbf{p}-\mathbf{q})^2(\mathbf{p}-\mathbf{k})^2} = \int \frac{d^Dp}{(2\pi)^D}\frac{\partial}{\partial p_\mu}\int d^Dx\,d^Dy\,d^Dz\,\frac{iy_\mu\,\mathrm{e}^{i[\mathbf{p}(\mathbf{x}+\mathbf{y}+\mathbf{z})-\mathbf{q}\mathbf{y}-\mathbf{k}\mathbf{z}]}}{(\mathbf{x}^2)^{D/2-1}(\mathbf{y}^2)^{D/2}(\mathbf{z}^2)^{D/2-1}}. \tag{13.33}$$

Carrying out the differentiation with respect to p_μ on the right-hand side produces a factor $(x+y+z)_\mu$. After the momentum integration, the right-hand side becomes

$$\int d^Dx\,d^Dy\,d^Dz\,\frac{ix_\mu\,(x+y+z)_\mu\,\delta^{(D)}(\mathbf{x}+\mathbf{y}+\mathbf{z})\,\mathrm{e}^{-i(\mathbf{q}\mathbf{y}+\mathbf{k}\mathbf{z})}}{(\mathbf{x}^2)^{D/2}(\mathbf{y}^2)^{D/2-1}(\mathbf{z}^2)^{D/2-1}} = 0. \tag{13.34}$$

Thus the surface term is indeed zero, and Eq. (13.32) is correct, which we now proceed to evaluate. Carrying out the momentum differentiation $\partial/\partial p_\mu(1/\mathbf{p}^2) \equiv \partial_{p_\mu}(1/\mathbf{p}^2) = -2p_\mu/\mathbf{p}^4$, we arrive at a sum of three integrals:

$$D\int\frac{d^Dp}{(2\pi)^D}\frac{1}{\mathbf{p}^2(\mathbf{p}-\mathbf{q})^2(\mathbf{p}-\mathbf{k})^2} = -\int\frac{d^Dp}{(2\pi)^D}\frac{1}{\mathbf{p}^2(\mathbf{p}-\mathbf{q})^2(\mathbf{p}-\mathbf{k})^2} \times\left[-2\frac{(p-q)_\mu p_\mu}{\mathbf{p}^2}-2\frac{(p-q)_\mu(p-q)_\mu}{(\mathbf{p}-\mathbf{q})^2}-2\frac{(p-q)_\mu(p-k)_\mu}{(\mathbf{p}-\mathbf{k})^2}\right]. \tag{13.35}$$

Let us represent the three integrals diagrammatically. A vertical dash on the line denotes a factor p_μ in the numerator, as defined in Eq. (11.49), whereas a dot symbolizes a ϕ^2-vertex insertion with a minus sign, as introduced in Eqs. (11.33) and (11.49), the latter implying an extra factor $\mathbf{p}^2$ in the denominator [recall (11.33)] .

D 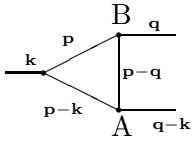

$= 2\left($ 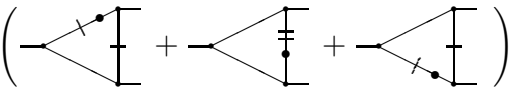 $+$ $+$ $\right).$ (13.36)

Momentum conservation at the upper and lower vertices of the diagrams leads to the following equations:

$$\begin{aligned} q_\mu = p_\mu-(p-q)_\mu &\Rightarrow -2(p-q)_\mu p_\mu = \mathbf{q}^2-\mathbf{p}^2-(\mathbf{p}-\mathbf{q})^2\\ (p-k)_\mu-(p-q)_\mu=(q-k)_\mu &\Rightarrow 2(p-q)_\mu(p-k)_\mu = (\mathbf{p}-\mathbf{q})^2+(\mathbf{p}-\mathbf{k})^2-(\mathbf{q}-\mathbf{k})^2. \end{aligned}$$

With their help we find an example of what will be refereed to as the *triangle rule* or *triangle relation* in momentum space, whose general form will be given in the next subsection:

$$\begin{aligned} D\int\frac{d^Dp}{(2\pi)^D}\frac{1}{\mathbf{p}^2(\mathbf{p}-\mathbf{q})^2(\mathbf{p}-\mathbf{k})^2} &= -\int\frac{d^Dp}{(2\pi)^D}\frac{1}{\mathbf{p}^2(\mathbf{p}-\mathbf{q})^2(\mathbf{p}-\mathbf{k})^2} \times\left[\frac{\mathbf{q}^2-\mathbf{p}^2-(\mathbf{p}-\mathbf{q})^2}{\mathbf{p}^2}-2-\frac{(\mathbf{p}-\mathbf{q})^2+(\mathbf{p}-\mathbf{k})^2-(\mathbf{q}-\mathbf{k})^2}{(\mathbf{p}-\mathbf{k})^2}\right]\\ &= -\int\frac{d^Dp}{(2\pi)^D}\frac{1}{\mathbf{p}^2(\mathbf{p}-\mathbf{q})^2(\mathbf{p}-\mathbf{k})^2}\left[-4+\frac{\mathbf{q}^2}{\mathbf{p}^2}+\frac{(\mathbf{q}-\mathbf{k})^2}{(\mathbf{p}-\mathbf{k})^2}-\frac{(\mathbf{p}-\mathbf{q})^2}{\mathbf{p}^2}-\frac{(\mathbf{p}-\mathbf{q})^2}{(\mathbf{p}-\mathbf{k})^2}\right]. \end{aligned} \tag{13.37}$$

A cancellation of squared momenta corresponds diagrammatically to the shrinking of a line. This equation may be applied to reduce all diagrams with triangles to nested simple loops. Note that the shrinking, and therefore the reduction, cannot be done for noninteger indices of the corresponding line. These arise by the integration of subdiagrams attached to the corresponding line, as mentioned in 13.2.

As an example, we apply the special triangle rule Eq. (13.37) to the KITE-type diagram.

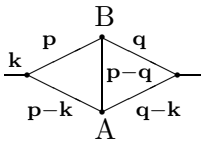

$$\begin{aligned} &= \int\frac{d^Dp}{(2\pi)^D}\frac{d^Dq}{(2\pi)^D}\frac{1}{\mathbf{p}^2\mathbf{q}^2(\mathbf{q}-\mathbf{k})^2(\mathbf{p}-\mathbf{k})^2(\mathbf{p}-\mathbf{q})^2}\\ &= \frac{1}{D-4}\int\frac{d^Dp}{(2\pi)^D}\frac{d^Dq}{(2\pi)^D}\frac{1}{\mathbf{p}^2(\mathbf{q})^2(\mathbf{q}-\mathbf{k})^2(\mathbf{p}-\mathbf{k})^2(\mathbf{p}-\mathbf{q})^2} \times\left[-\frac{\mathbf{q}^2}{\mathbf{p}^2}-\frac{(\mathbf{q}-\mathbf{k})^2}{(\mathbf{p}-\mathbf{k})^2}+\frac{(\mathbf{p}-\mathbf{q})^2}{\mathbf{p}^2}+\frac{(\mathbf{p}-\mathbf{q})^2}{(\mathbf{p}-\mathbf{k})^2}\right]. \end{aligned} \tag{13.38}$$

The symmetry of the diagram allows the replacement of the integration variables $\mathbf{p}$ by $\mathbf{p}-\mathbf{k}$, and $\mathbf{q}$ by $\mathbf{q}-\mathbf{k}$, so that we end up with two integrals

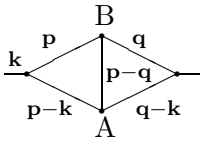

$$= \frac{2}{D-4}\int\frac{d^Dp}{(2\pi)^D}\frac{d^Dq}{(2\pi)^D}\left[-\frac{1}{\mathbf{p}^2(\mathbf{p}-\mathbf{k})^4\mathbf{q}^2(\mathbf{p}-\mathbf{q})^2}+\frac{1}{\mathbf{p}^2(\mathbf{p}-\mathbf{k})^4\mathbf{q}^2(\mathbf{q}-\mathbf{k})^2}\right]. \tag{13.39}$$

The right-hand side corresponds to two diagrams with shrunk lines:

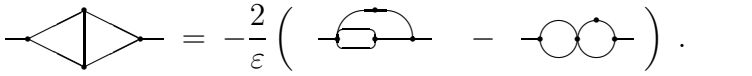

$$= -\frac{2}{\varepsilon}\Big(\quad - \quad \Big) . \tag{13.40}$$

Thus the generic two-loop diagram of the KITE type has been reduced to two primitive diagrams with one line index raised by one unit.

13.4.2 General Triangle Rule

The reduction of the triangle integral will be reformulated as a general relation which is applicable to the reduction of all diagrams containing a triangle subdiagram. The general index configuration is specified in Fig. 13.4. Triangle subdiagrams occur in diagrams of the KITE, LADDER, and BENZ type. The method consists in finding all those identities of the type (13.31) which lead to independent reduction formulas of the type (13.37). For this purpose, a generalized differentiation with respect to a loop momentum is introduced. In $\mathbf{x}$-space, the differentiation with respect to the loop momentum generates a factor containing the differences of initial and final coordinates of each line in the loop integral, which add up to zero.

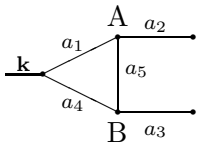

FIGURE 13.4 Subdiagram for the KITE-Type reduction formula.

The integral for the triangle diagram in Fig. 13.4 is denoted by $\mathrm{T}(a_1,a_2,a_3,a_4,a_5)$, where a_i are the line indices. Let $\mathbf{p}_i$ be the momenta with line indices a_i. For the moment we assume all momenta to be independent, ignoring momentum conservation at the vertices, i.e., we associate each line with a momentum of its own. In each diagram, there are three integrals to which the three lines of the triangular subdiagram contribute. Now we introduce the operation of differentiation with respect to a closed oriented loop $\mathbf{L}$. For the triangle diagram we define the set of loop momenta and the associated loop derivative:

$$\mathbf{L} = \{\mathbf{p}_1,\mathbf{p}_5,\mathbf{p}_4\}, \qquad \partial_{\mathbf{L}} = \frac{\partial}{\partial\mathbf{p}_1}+\frac{\partial}{\partial\mathbf{p}_5}+\frac{\partial}{\partial\mathbf{p}_4}, \tag{13.41}$$

where the sign is determined by the orientation of the loop, here clockwise. A vector is chosen

$$\mathbf{P} = \left(\sum_i b_i\,\mathbf{p}_i\right) + b\mathbf{k}, \tag{13.42}$$

with arbitrary numbers b_i and b, and momenta $\mathbf{p}_i$ of the subdiagram in Fig. 13.4. Since there are three independent loop momenta, or two loop momenta and one external momentum, there is a

three-dimensional manifold of choices for $\mathbf{P}$, from which we may pick three linearly independent ones.

A reduction formula for a diagram which contains the triangle is now found from an identity which expresses the vanishing of the surface term:

$$\partial_{\mathbf{L}} \cdot \mathbf{P} \ \mathrm{T}\ (a_1, a_2, a_3, a_4, a_5) = 0\ , \tag{13.43}$$

this being a generalization of Eq. (13.33). The operation in (13.43) is understood to be performed *inside* the integral over the closed oriented loop Ł.

This identity holds not only for the triangle diagram itself, but also for any loop integral containing a triangle subdiagram with the loop vector $\mathbf{P}$.

As an example consider the integral of the KITE type. This contains two independent loop momenta and one external momentum, giving three possible independent vectors $\mathbf{P}$. With the two independent loops, we can construct six independent equations. In general, their number is $(L+1) \times L$. Three other equations are generated by closing the external momenta to form an additional loop $\mathbf{L} = \{\mathbf{k}, \mathbf{p}_1, \mathbf{p}_2\}$. For $\mathbf{P} = \mathbf{k}$, the technical dimension of the integrals $d_t = 2(D - \sum_{i=1}^{I} a_i)$ allows us to conclude that the function $\mathrm{KI}(a_i)$ resulting from the two-loop integral of the KITE type satisfies the identity

$$d_t \mathrm{KI}\,(a_i) = \left(\mathbf{k}\frac{\partial}{\partial \mathbf{k}}\right) \mathrm{KI}\,(a_i) = -\mathbf{k}\left(\frac{\partial}{\partial \mathbf{p}_1} + \frac{\partial}{\partial \mathbf{p}_2}\right) \mathrm{KI}\,(a_i)\ . \tag{13.44}$$

There exist nine independent equations of this type.

The algorithm for the KITE-type integral treated in detail as an example on page 236, is expressed in this notation by choosing $\mathbf{L} = \{\mathbf{p}_1, \mathbf{p}_5, \mathbf{p}_4\}$, $\mathbf{P} = \mathbf{p}_5$:

$$\begin{aligned} \mathrm{KI}\,(a_1, a_2, a_3, a_4, a_5) = {} & (-2a_5 - a_1 - a_4 + D)^{-1} \times \\ & \Big[\ a_1 \Big\{ \mathrm{KI}\,(a_1 + 1, a_2, a_3, a_4, a_5 - 1) - \mathrm{KI}\,(a_1 + 1, a_2 - 1, a_3, a_4, a_5) \Big\} \\ & + a_4 \Big\{ \mathrm{KI}\,(a_1, a_2, a_3, a_4 + 1, a_5 - 1) - \mathrm{KI}\,(a_1, a_2, a_3 - 1, a_4 + 1, a_5) \Big\} \Big]\ . \end{aligned} \tag{13.45}$$

This formula leads to a reduction to nested simple loops if the line indices a_2, a_3, and a_5 are integer. It reduces to Eqs. (13.38) and (13.39) for $a_i = 1$. An analogous reduction can be performed with all diagrams of LADDER and BENZ types in Fig. 13.1, since these contain triangular subdiagrams.

For line indices satisfying the relation $2a_5 + a_1 + a_4 = 4 + \mathcal{O}(\varepsilon)$, the above reduction of $\mathrm{KI}\,(a_1, \ldots)$ produces a pole in ε multiplied by a combination of primitive two-loop diagrams. We may express this schematically as

$$\mathrm{KI}\,(a_1, \ldots) = \frac{1}{\varepsilon} \sum a_i\, L(a_k, a_l) \times L(a_p, a_q)\,, \quad \text{for} \quad 2a_5 + a_1 + a_4 = 4 + \mathcal{O}(\varepsilon)\,. \tag{13.46}$$

A similar property is shared by all formulas derived by partial integration. The pole requires an expansion of the loop functions $L(a, b)$ to higher orders.

Repeated application of the reduction formula (13.43) allows us to reduce any integer line index a_2, a_3, or a_5 to zero. This is possible for arbitrary line indices a_1, a_4. The restriction to integer line indices is important. A zero index corresponds to shrinking the corresponding line, and results in a primitive diagram. Insertions of primitive loops which give rise to noninteger line indices should therefore lie on the lines 1 and 4. Unfortunately, the so-called special KITE type, $\mathrm{KI}\,(a_1, \ldots, n + m\varepsilon)$, with $a_1, \ldots, a_4$ integer, cannot be reduced by the algorithm. This

type is encountered when reducing generic three-loop diagrams. It has to be calculated by other methods.

For generic four- and five-loop diagrams, no reduction algorithms are at present available. The reason is the appearance of more complicated subdiagrams than triangle diagrams, for example the square subdiagram, which cannot be reduced by partial integration.

The only type of generic diagrams in Fig. 13.1 where the triangle rule cannot be used is the NONPLANAR type, which does not contain any triangle. But it can be applied to the diagrams LADDER and BENZ. The algorithms found for these two correspond to each other if the line indices are mapped as in Fig. 13.5. The so-called *mapping* [1] transforms the external

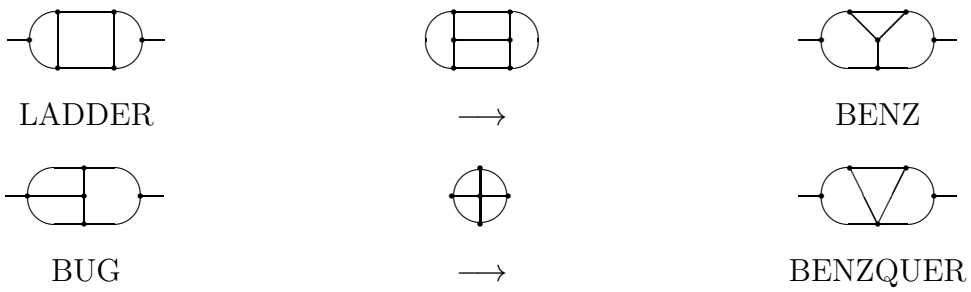

FIGURE 13.5 Mapping of generic three-loop diagrams LADDER and BENZ, and of three-loop diagrams BUG and BENZQUER, which are generated in the reduction of BENZ and LADDER in Fig. 13.4.3.

momentum into a loop momentum by identifying its ends to a new loop (see Fig. 13.5). This representation gives full account to the integral's invariance under differentiation with respect to the external momentum as well as with respect to the loop momentum. The momentum conservation at each single vertex is unchanged even if the diagram is cut at a different line. Like the vectors $\mathbf{P}$ and the loops $\mathbf{L}$, the $(L+1)$ equations of the two diagrams can also be transformed into one another by mapping. The same relationship holds for the two diagrams which emerge from one of the generic diagrams listed above by shrinking a line, as can be seen in Fig. 13.5. The reduction formulas for these diagrams, the BEQ and the BUG type, follow from those of the LA or the BE type by setting to zero the corresponding line index.

13.4.3 Reduction Algorithms

The levels of reduction for the generic three-loop diagrams LA and BE will now be displayed explicitly. The algorithms transform the diagrams of level I into those of level II and III (see Fig. 13.6). Those of level II are further reduced to level III and primitive diagrams. The diagrams of level III are reduced to primitive diagrams. The diagram ONE1 cannot be reduced, but can be reduced to the standard expression $\mathrm{KI}(1,1,1,1,m\varepsilon/2)L(1,1)$.

The following reduction algorithms [4] are used in our calculation. The algorithms reduce the integral types KITE, LADDER, BENZ and BENZQUER algebraically to primitive integrals and to the special KITE type. They also reduce the special KITE type $\mathrm{KI}\,(n_1,n_2,n_3,n_4,n_5+m\varepsilon/2)$ with n_i, m integer to the standard form. Other algorithms to bring the NO integral to its standard form with $a_i = 1$ are not listed here. They have not been used in the five-loop calculations because the only time the NO type appears it does so in the standard form.

The notation corresponds to the listing of the diagrams on page 240, the additional

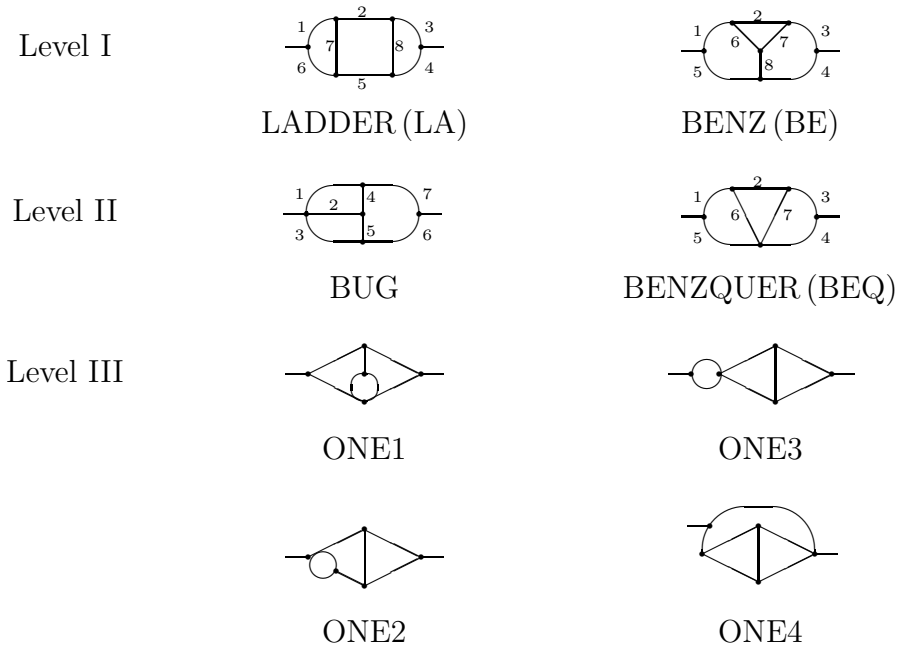

FIGURE 13.6 The diagrams which are generated in the reduction of LADDER- and BUG-type diagrams. The reduction works from Level I down to level III. Application of the reduction algorithms for the KITE-type to the diagrams of level III leads to primitive diagrams.

generation of primitive diagrams of level II and for the KITE type is not explicitly stated. The results are:

LADDER: $\mathrm{LA} = \mathcal{O}(1/\varepsilon)\,\mathrm{BEQ} + \mathcal{O}(1/\varepsilon)\,\mathrm{ONE3}, \quad a_2,\ a_5,\ a_8$ integer.

$$\begin{aligned}\mathrm{LA}(a_1,\ldots,a_8) &= (D-2a_8-a_3-a_4)^{-1}\times \\ &\Big[\ a_4\mathrm{LA}(a_1,a_2,a_3,a_4+1,a_5,a_6,a_7,a_8-1) \\ &- a_4\mathrm{LA}(a_1,a_2,a_3,a_4+1,a_5-1,a_6,a_7,a_8) \\ &+ a_3\mathrm{LA}(a_1,a_2,a_3+1,a_4,a_5,a_6,a_7,a_8-1) \\ &- a_3\mathrm{LA}(a_1,a_2-1,a_3+1,a_4,a_5,a_6,a_7,a_8)\Big]\end{aligned} \tag{13.47}$$

BENZ: $\mathrm{BE} = \mathcal{O}(1/\varepsilon)\,\mathrm{BUG} + \mathcal{O}(1/\varepsilon)\,\mathrm{ONE1}, \quad a_1,\ a_2,\ a_3$ integer.

$$\begin{aligned}\mathrm{BE}(a_1,\ldots,a_8) &= (D-2a_2-a_6-a_7)^{-1}\times \\ &\Big[\ a_6\mathrm{BE}(a_1,a_2-2,a_3,a_4,a_5,a_6+1,a_7,a_8) \\ &- a_6\mathrm{BE}(a_1-1,a_2,a_3,a_4,a_5,a_6+1,a_7,a_8) \\ &+ a_7\mathrm{BE}(a_1,a_2-1,a_3,a_4,a_5,a_6,a_7+1,a_8) \\ &- a_7\mathrm{BE}(a_1,a_2,a_3-1,a_4,a_5,a_6,a_7+1,a_8)\Big]\end{aligned} \tag{13.48}$$

BENZQUER: $\mathrm{BEQ} = \mathcal{O}(1/\varepsilon)\,\mathrm{ONE1} + \mathcal{O}(1/\varepsilon)\,\mathrm{ONE2}, \qquad a_1,\, a_2,\, a_3$ integer.

$$\mathrm{BEQ}(a_1,\ldots,a_7) \;=\; \mathrm{BENZ}(a_1,\ldots,a_7,0) \tag{13.49}$$

BUG: $\mathrm{BUG} = \mathcal{O}(1/\varepsilon)\,\mathrm{ONE2} + \mathcal{O}(1/\varepsilon)\,\mathrm{ONE4}, \quad a_2,\, a_4,\, a_5,\, a_7$ integer.

$$\begin{aligned}\mathrm{BUG}(a_1,\ldots,a_8) \;=\; & (D-2a_5-a_2-a_3)^{-1}\times \\ & \Big[\; a_2\mathrm{BU}(a_1,a_2+1,a_3,a_4,a_5-1,a_6,a_7,a_8) \\ & - a_2\mathrm{BU}(a_1,a_2+1,a_3,a_4-1,a_5,a_6,a_7,a_8) \\ & + a_3\mathrm{BU}(a_1,a_2,a_3+1,a_4,a_5-1,a_6,a_7,a_8) \\ & - a_3\mathrm{BU}(a_1,a_2-1,a_3+1,a_4,a_5,a_6,a_7-1,a_8)\Big]\end{aligned} \tag{13.50}$$

KITE-TYPE: $\mathrm{KI} = \mathcal{O}(1/\varepsilon)\times L\times L, \quad a_2,\, a_3,\, a_5$ integer.

$$\begin{aligned}\mathrm{KI}\,(a_1,\ldots,a_5) \;=\; & (D-2a_5-a_1-a_4)^{-1}\times \\ & \Big[\; a_1\mathrm{KI}\,(a_1+1,a_2,a_3,a_4,a_5-1) \\ & - a_1\mathrm{KI}\,(a_1+1,a_2-1,a_3,a_4,a_5) \\ & + a_4\mathrm{KI}\,(a_1,a_2,a_3,a_4+1,a_5-1) \\ & - a_4\mathrm{KI}\,(a_1,a_2,a_3-1,a_4+1,a_5)\Big]\end{aligned} \tag{13.51}$$

SPECIAL KITE-TYPE:

$$\mathrm{KI}\,(a_1,\ldots,a_4,n+\tfrac{m}{2}\varepsilon) = \mathcal{O}(1/\varepsilon)\,\mathrm{KI}\,(1,1,1,1,n+\tfrac{m}{2}\varepsilon)\;,\; a_1,\ldots,a_4,m,n \text{ integer.}$$

$$\begin{aligned}(a_4-1)\mathrm{KI}\,(a_1,a_2,a_3,a_4,a_5) \;=\; & \Big[(2a_1+a_4+a_5-D-1)\mathrm{KI}\,(a_1,a_2,a_3,a_4-1,a_5) \\ & + (a_4-1)\mathrm{KI}\,(a_1-1,a_2,a_3,a_4,a_5) \\ & + a_5\Big\{\mathrm{KI}\,(a_1-1,a_2,a_3,a_4-1,a_5+1) \\ & \qquad - \mathrm{KI}\,(a_1,a_2-1,a_3,a_4-1,a_5+1)\Big\}\Big]\end{aligned} \tag{13.52}$$

$$\begin{aligned}\mathrm{KI}\,(1,1,1,1,a_5) \;=\; & (a_5+2-D)(a_5+1-D/2)^{-1}\mathrm{KI}\,(1,1,1,1,a_5-1) \\ & + 2(3D-10-2a_5)L(1,a_5)\,L(1,a_5+2-D/2).\end{aligned} \tag{13.53}$$

These algorithms allow us to find analytic expression for the divergent part of all four-loop diagrams, and of most of the five-loop diagrams of the ϕ^4-theory once $\mathrm{KI}\,(1,1,1,1,m\varepsilon/2)$ is calculated to a sufficient order in ε, which will be done in the next section.

The five-loop diagrams which cannot yet be calculated in this manner contain either generic four-loop diagrams or subdiagrams of the NONPLANAR type. They will be shown in Fig. 13.10. The expansion for $\mathrm{KI}\,(1,1,1,1,m\varepsilon/2)$ is given in the next section in Eq. (13.75). It cannot be calculated with the momentum space methods presented so far. The same problem exists for the BUG- and BEQ-type integrals with noninteger line indices. Fortunately, up to five loops the calculation of the last two can be circumvented using an appropriate infrared rearrangement, and removing the spurious IR-divergences.

A direct calculation of these diagrams is possible in configuration space. This was first done numerically with the help of the so-called *Gegenbauer polynomial* $\mathbf{x}$*-space method* [2]. Each propagator is expanded into a set of orthogonal polynomials, the Gegenbauer polynomials. Integration were carried out resulting in multiple series, which were summed numerically on a computer.

Analytical expressions were finally found by the *method of ideal index constellations*, which was developed by Kazakov [3] and which will now be explained.

13.5 Method of Ideal Index Constellations in Configuration Space

The method [3, 9] consists of the combined application of several characteristic identities to diagrams with certain ideal line index constellations. To reach such constellations, the indices are manipulated, after a Fourier transformation, by a configuration space version of the triangle rule of the last section, or by the insertion of a ϕ^2-vertex. This method succeeds in giving analytic expressions for the missing diagrams up to fifth order in ε. An important tool among the following methods is the *duality transformation*.

13.5.1 Dual Diagrams

In Eq. (13.2), we have observed that the Fourier transformation of a massless propagator yields a pure power in $\mathbf{x}$. This has the pleasant consequence that the Fourier transform of an arbitrary massless Feynman integral is again a massless Feynman integral, but has a different mathematical form and is expressed in terms of $\mathbf{x}$ instead of $\mathbf{p}$. If this $\mathbf{x}$-space integral is diagrammatically represented in the same way as a $\mathbf{p}$-space integral, the resulting diagram will be called the *dual Feynman diagram*. It is obvious, that the propagator-type integral of a diagram and the $\mathbf{x}$-space integral of its dual diagram are of the same form. The line indices α of the dual diagram are related to the indices a of the original one by $\alpha = D/2 - a$. Examples for dual diagrams are shown in Fig. 13.7, the integrals of the BUG and the BEQ type are dual to each other, while the integral of the KITE type is dual to itself.

$$\sim \int \frac{d^D p}{(2\pi)^D \mathbf{p}^{2a} (\mathbf{p}-\mathbf{k})^{2b}} \qquad \int \frac{d^D x\, \mathrm{e}^{i\mathbf{kx}}}{(\mathbf{x}^2)^{\alpha+\beta}}$$

$$\sim \int \frac{d^D p\, \mathrm{e}^{-i\mathbf{px}}}{(2\pi)^D (\mathbf{p}^2)^{a+b}} \qquad \int \frac{d^D x}{\mathbf{x}^{2\alpha} (\mathbf{x}-\mathbf{y})^{2\beta}}$$

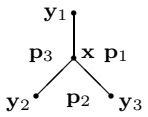

$$\sim \int \frac{(2\pi)^{-3D} d^D p_2\, d^D p_2\, d^D p_3}{(\mathbf{p}_1-\mathbf{p}_3)^{2a} (\mathbf{p}_2-\mathbf{p}_3)^{2b} (\mathbf{p}_1-\mathbf{p}_2)^{2c}} \qquad \int \frac{d^D x}{(\mathbf{x}-\mathbf{y}_1)^{2\alpha} (\mathbf{x}-\mathbf{y}_2)^{2\beta} (\mathbf{x}-\mathbf{y}_3)^{2\gamma}}$$

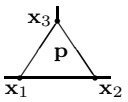

$$\sim \int \frac{d^D p}{(2\pi)^D \mathbf{p}^{2a} (\mathbf{p}-\mathbf{q})^{2b} (\mathbf{p}-\mathbf{k})^{2c}} \qquad \int \frac{d^D x_1\, d^D x_2\, d^D x_3}{(\mathbf{x}_1-\mathbf{x}_3)^{2\alpha} (\mathbf{x}_2-\mathbf{x}_3)^{2\beta} (\mathbf{x}_1-\mathbf{x}_2)^{2\gamma}}$$

FIGURE 13.7 The $\mathbf{p}$- and $\mathbf{x}$-space representations of the integrals and the corresponding diagrams. The first two diagrams are dual to each other and so are the last two. The $\mathbf{x}$-space integral corresponds mathematically to the $\mathbf{p}$-space integral of the dual diagram and vice versa.

Loops and Chains

Repeating here the Fourier transformation of the simple loop of Eqs. (13.3) and (13.4),

$$\sim \int \frac{d^D p}{(2\pi)^D} \frac{1}{(\mathbf{p}^2)^a [(\mathbf{p}-\mathbf{k})^2]^b} \tag{13.54}$$

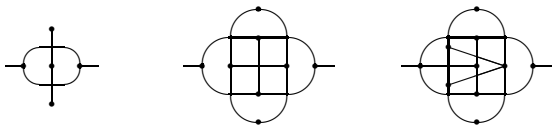

FIGURE 13.8 Construction of dual diagrams

$$= \frac{\Gamma(D/2-a)\Gamma(D/2-b)}{\pi^D\Gamma(a)\Gamma(b)4^{a+b}} \int d^Dx \, \frac{\mathrm{e}^{i\mathbf{kx}}}{[(\mathbf{x})^2]^{D/2-a}[(\mathbf{x})^2]^{D/2-b}} \,, \tag{13.55}$$

we see that the convolution integral with the diagrammatic representation of a loop is transformed in **x**-space into a product of two identical propagators, causing a collapse of the two lines to a single line whose index is the sum of the original line indices. If the resulting **x**-space integral is represented diagrammatically as if it were a **p**-space integral, we have the dual diagram:

$$\overset{\alpha_1}{\bullet}\!\!-\!\!\bullet\!\!-\!\!\bullet\overset{\alpha_2}{} \;\sim\; \frac{1}{[(\mathbf{x})^2]^{\alpha_1}[(\mathbf{x})^2]^{\alpha_2}} = \frac{1}{[(\mathbf{x})^2]^{\alpha_1+\alpha_2}} \;\sim\; \overset{\alpha_1+\alpha_2}{\bullet\!\!-\!\!\bullet} \,. \tag{13.56}$$

The diagram on the left-hand side is called a *chain diagram*. We can also start from the propagator-type integral of the chain diagram, in which case we have to go in the opposite direction from (13.55) to (13.54). If the chain has one link, as in this case, the **x**-space representation corresponds to a convolution integral of the type (13.54), which can be calculated with the same result as the loop integral (13.4) in momentum space:

$$\int d^Dy \frac{1}{[(\mathbf{x}-\mathbf{y})^2]^{\alpha_1}[(\mathbf{y}-\mathbf{z})^2]^{\alpha_2}} = \pi^{D/2} \, \frac{\nu(\alpha_1)\nu(\alpha_2)\nu(D-\alpha_1-\alpha_2)}{[(\mathbf{x}-\mathbf{z})^2]^{(\alpha_1+\alpha_2-D/2)}} \,. \tag{13.57}$$

Another type of diagram arising from the duality transformation of the **p**-space triangle diagram in Fig. 13.7 is an integral over the variable $\mathbf{x}$ of a ϕ^3-vertex. It is called a *star diagram* and the corresponding integral in **x**-space reads

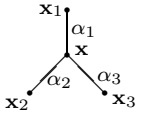

$$\hat{=} \quad \int d^Dx \, \frac{1}{[(\mathbf{x}-\mathbf{x}_1)^2]^{\alpha_1}[(\mathbf{x}-\mathbf{x}_2)^2]^{\alpha_2}[(\mathbf{x}-\mathbf{x}_3)^2]^{\alpha_3}} \,. \tag{13.58}$$

As visible in Fig. 13.7, this **x**-space integral has the same form as the momentum space triangle integral in Eq. (13.32) except for the indices, and it can also be treated by the reduction formula (13.37) found for diagrams of this form. The star diagram will be considered further in the next subsection.

Generally, the dual diagram is constructed by placing a vertex into each loop and outside of it, and connecting them in such a way that each line of the original diagram is crossed once. In this way one vertex is associated with each loop. This corresponds to the transition from loop integration to **x**-integration in the Fourier transformation. In momentum space, the lines in chain diagrams collapse when adding the indices. In **x**-space, the same thing happens for the lines of the simple loop.

We will see that the duality transformation is sometimes helpful in creating calculable diagrams.

13.5.2 Star-Triangle Rule for an Ideal Vertex

The **x**-space integral for the star diagram

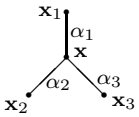

$$\hat{=} \quad \int d^Dx \, \frac{1}{[(\mathbf{x}-\mathbf{x}_1)^2]^{\alpha_1}[(\mathbf{x}-\mathbf{x}_2)^2]^{\alpha_2}[(\mathbf{x}-\mathbf{x}_3)^2]^{\alpha_3}} \tag{13.59}$$

is simplified if one of the line indices is zero, thus producing a chain. Another simplification occurs for index constellations with $\sum \alpha_i = D$, in which case we speak of an *ideal vertex*. The simplification is the content of the *star-triangle rule*, which is derived as follows. Translation of the variable of integration $\mathbf{x} \to \mathbf{x}' = \mathbf{x} + \mathbf{x}_1$ gives

$$\int d^D x \, \frac{1}{(\mathbf{x}^2)^{\alpha_1}[(\mathbf{x}+\mathbf{x}_1-\mathbf{x}_2)^2]^{\alpha_2}[(\mathbf{x}+\mathbf{x}_1-\mathbf{x}_3)^2]^{\alpha_3}} \; . \tag{13.60}$$

Inversion of the variables of integration: $\mathbf{x} \to \mathbf{x}' = \mathbf{x}/\mathbf{x}^2$, $d^D x \to d^D x' = d^D x/(\mathbf{x}^2)^D$ such that

$$[(\mathbf{x}-\mathbf{y})^2]^\alpha \; \to \; \left[\left(\frac{\mathbf{x}}{\mathbf{x}^2}-\mathbf{y}\right)^2\right]^\alpha = \frac{(1-2\mathbf{x}\mathbf{y}+\mathbf{x}^2\mathbf{y}^2)^\alpha}{(\mathbf{x}^2)^\alpha} = \frac{[(\mathbf{x}-\frac{\mathbf{y}}{\mathbf{y}^2})^2]^\alpha (\mathbf{y}^2)^\alpha}{(\mathbf{x}^2)^\alpha}, \tag{13.61}$$

results in

$$\int d^D x \, \frac{1}{(\mathbf{x}^2)^D} \left\{ \left(\frac{\mathbf{x}^2}{\mathbf{x}^4}\right)^{\alpha_1} \left[\frac{\left(\mathbf{x}-\frac{\mathbf{x}_1-\mathbf{x}_2}{(\mathbf{x}_1-\mathbf{x}_2)^2}\right)^2 (\mathbf{x}_1-\mathbf{x}_2)^2}{\mathbf{x}^2}\right]^{\alpha_2} \left[\frac{\left(\mathbf{x}-\frac{\mathbf{x}_1-\mathbf{x}_3}{(\mathbf{x}_1-\mathbf{x}_3)^2}\right)^2 (\mathbf{x}_1-\mathbf{x}_3)^2}{\mathbf{x}^2}\right]^{\alpha_3} \right\}^{-1}$$

$$= \int d^D x \left[(\mathbf{x}^2)^{D-\alpha_1-\alpha_2-\alpha_3} \left[\left(\mathbf{x}-\frac{\mathbf{x}_1-\mathbf{x}_2}{(\mathbf{x}_1-\mathbf{x}_2)^2}\right)^2\right]^{\alpha_2} \left[\left(\mathbf{x}-\frac{\mathbf{x}_1-\mathbf{x}_3}{(\mathbf{x}_1-\mathbf{x}_3)^2}\right)^2\right]^{\alpha_3} [(\mathbf{x}_1-\mathbf{x}_2)^2]^{\alpha_2} [(\mathbf{x}_1-\mathbf{x}_3)^2]^{\alpha_3}\right]^{-1}.$$

For $\sum \alpha_i = D$ the line index of $\mathbf{x}^2$ vanishes, and we are left with

$$\int d^D x \left\{ \left[\left(\mathbf{x}-\frac{\mathbf{x}_1-\mathbf{x}_2}{(\mathbf{x}_1-\mathbf{x}_2)^2}\right)^2\right]^{\alpha_2} \left[\left(\mathbf{x}-\frac{\mathbf{x}_1-\mathbf{x}_3}{(\mathbf{x}_1-\mathbf{x}_3)^2}\right)^2\right]^{\alpha_3} \left[(\mathbf{x}_1-\mathbf{x}_2)^2\right]^{\alpha_2} \left[(\mathbf{x}_1-\mathbf{x}_3)^2\right]^{\alpha_3} \right\}^{-1}.$$

The integration over $\mathbf{x}$ is a chain integration which may be carried out with the help of Eq. (13.57) leading to

$$\frac{\pi^{D/2} \; \nu(\alpha_1) \, \nu(\alpha_2) \, \nu(\alpha_3)}{\left[\left(\frac{\mathbf{x}_1-\mathbf{x}_2}{(\mathbf{x}_1-\mathbf{x}_2)^2}-\frac{\mathbf{x}_1-\mathbf{x}_3}{(\mathbf{x}_1-\mathbf{x}_3)^2}\right)^2\right]^{\alpha_2+\alpha_3-\frac{D}{2}} [(\mathbf{x}_1-\mathbf{x}_2)^2]^{\alpha_2} [(\mathbf{x}_1-\mathbf{x}_3)^2]^{\alpha_3}} \; . \tag{13.62}$$

With

$$D = \alpha_1+\alpha_2+\alpha_3 \Rightarrow \left\{ \begin{array}{lcl} \alpha_2 & = & (\frac{D}{2}-\alpha_3)+(\frac{D}{2}-\alpha_1) \\ \alpha_3 & = & (\frac{D}{2}-\alpha_2)+(\frac{D}{2}-\alpha_1) \\ \alpha_2+\alpha_3-\frac{D}{2} & = & \frac{D}{2}-\alpha_1 \end{array} \right. , \tag{13.63}$$

this can be rewritten to:

$$\frac{\pi^{D/2} \; \nu(\alpha_1) \, \nu(\alpha_2) \, \nu(\alpha_3)}{\left[\left(\frac{\mathbf{x}_1-\mathbf{x}_2}{(\mathbf{x}_1-\mathbf{x}_2)^2}-\frac{\mathbf{x}_1-\mathbf{x}_3}{(\mathbf{x}_1-\mathbf{x}_3)^2}\right)^2\right]^{\frac{D}{2}-\alpha_1} [(\mathbf{x}_1-\mathbf{x}_2)^2]^{\frac{D}{2}-\alpha_1} [(\mathbf{x}_1-\mathbf{x}_3)^2]^{\frac{D}{2}-\alpha_1} [(\mathbf{x}_1-\mathbf{x}_2)^2]^{\frac{D}{2}-\alpha_3} [(\mathbf{x}_1-\mathbf{x}_3)^2]^{\frac{D}{2}-\alpha_2}} \; .$$

Finally, we obtain the star-triangle rule:

$$\int \frac{d^D x}{[(\mathbf{x}-\mathbf{x}_1)^2]^{\alpha_1}[(\mathbf{x}-\mathbf{x}_2)^2]^{\alpha_2}[(\mathbf{x}-\mathbf{x}_3)^2]^{\alpha_3}}$$

$$\stackrel{\sum \alpha_i = D}{=} \frac{\pi^{D/2} \; \nu(\alpha_1) \, \nu(\alpha_2) \, \nu(\alpha_3)}{[(\mathbf{x}_2-\mathbf{x}_3)^2]^{\frac{D}{2}-\alpha_1}[(\mathbf{x}_1-\mathbf{x}_2)^2]^{\frac{D}{2}-\alpha_3}[(\mathbf{x}_1-\mathbf{x}_3)^2]^{\frac{D}{2}-\alpha_2}} \; . \tag{13.64}$$

This relation allows us to carry out the integration over ϕ^3-vertices (stars) if their indices satisfy $\sum \alpha_i = D$. The diagrammatic expression is

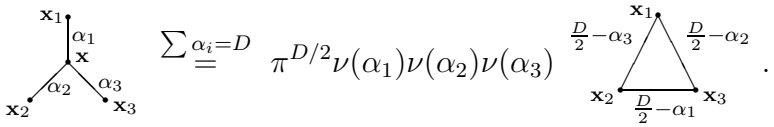

An ideal index constellation admits a simple integration and exists for the star, the triangle, and the chain:

$$\text{A} \left\{ \begin{array}{l} \text{line} \\ \text{vertex} \\ \text{triangle} \end{array} \right\} \quad \text{is ideal if} \quad \left\{ \begin{array}{lcl} \alpha & = & 0 \\ \sum \alpha_i & = & D \\ \sum \alpha_i & = & D/2 \end{array} \right. . \tag{13.65}$$

The star-triangle relation transforms an ideal vertex into an ideal triangle. A diagram containing such a vertex can thereby be reduced to primitive diagrams. For example, the application of the star-triangle relation reduces the KITE type to a primitive diagram if a vertex or a triangle is ideal. For the KITE-type diagram in **x**-space, we find

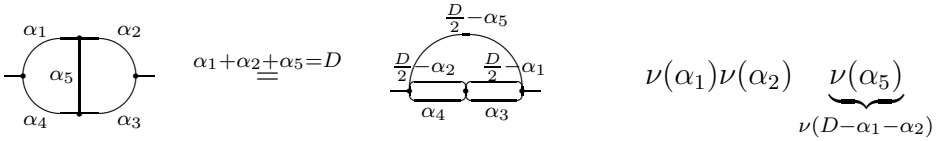

(13.66)

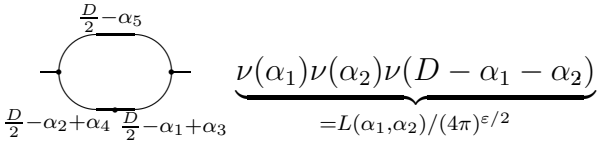

(13.67)

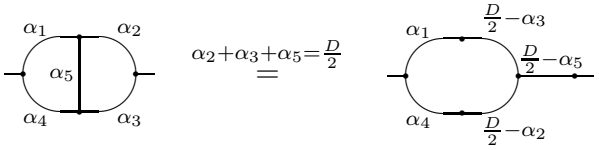

(13.68)

$$\Big[L(\tfrac{D}{2}-\alpha_2,\tfrac{D}{2}-\alpha_3) \overset{\alpha_2+\alpha_3+\alpha_5=\frac{D}{2}}{=} \nu(\tfrac{D}{2}-\alpha_2)\nu(\tfrac{D}{2}-\alpha_3)\nu(\tfrac{D}{2}-\alpha_5) = \nu^{-1}(\alpha_2)\nu^{-1}(\alpha_3)\nu^{-1}(\alpha_5) \Big] . \tag{13.69}$$

The resulting diagrams are primitive **x**-space diagrams, and can be calculated using Eqs. (13.56) and (13.57). Transformation to momentum space converts loops into chains and vice versa.

13.5.3 One Step from Ideal Index Constellation

In momentum space the method of partial integration has led to the reduction formula (13.37) for the triangle integral. We are now going to transform this relation into **x**-space where the triangle integral becomes an integral of the star type:

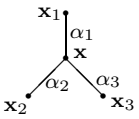

$$\hat{=} \quad \int \frac{d^D x}{[(\mathbf{x}-\mathbf{x}_1)^2]^{\alpha_1}[(\mathbf{x}-\mathbf{x}_2)^2]^{\alpha_2}[(\mathbf{x}-\mathbf{x}_3)^2]^{\alpha_3}} , \tag{13.70}$$

and the triangle relation (13.37) takes the following form:

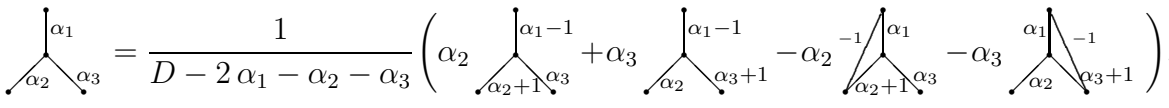

(13.71)

This relation can be used for any arrangement of indices, but for particular ones it simplifies considerably. If the vertex on the left-hand side of (13.71) is *one step from ideal*, i.e. if the indices satisfy $\alpha_1+\alpha_2+\alpha_3 = D-1$, the relation turns into

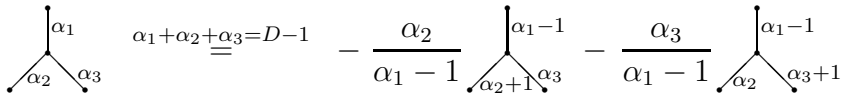

$$- \frac{\alpha_2}{\alpha_1-1} - \frac{\alpha_3}{\alpha_1-1} \tag{13.72}$$

$$+ \alpha_2\alpha_3\nu(\alpha_1)\nu(\alpha_2+1)\nu(\alpha_3+1)$$

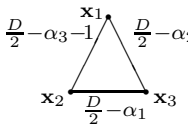

,

where we used $\alpha_2\alpha_3\nu(\alpha_1)\nu(\alpha_2+1)\nu(\alpha_3+1) = \frac{\alpha_2}{\alpha_1-1}\nu(\alpha_1)\nu(\alpha_2+1)\nu(\alpha_3) + \frac{\alpha_3}{\alpha_1-1}\nu(\alpha_1)\nu(\alpha_2)\nu(\alpha_3+1)$. If, in addition, both triangles are one step from an ideal index constellation $D/2+1$, this relation transforms the KITE-type diagram into integrable diagrams. For indices of the form $\alpha_i = 1+c_i$ we have $\alpha_3+\alpha_4+\alpha_5 = D-1$, $\alpha_1+\alpha_4+\alpha_5 = D/2+1$, and $\alpha_2+\alpha_3+\alpha_5 = D/2+1$, such that:

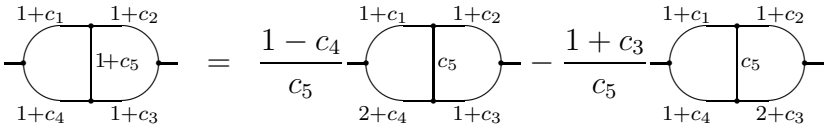

$$= \frac{1-c_4}{c_5} - \frac{1+c_3}{c_5} \tag{13.73}$$

$$+(1+c_3)(1+c_4)\nu(1+c_5)\nu(2+c_3)\nu(2+c_4)$$

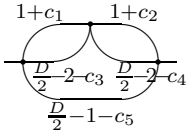

.

The first diagram on the right-hand side can now be integrated because the right triangle has got an ideal index constellation. In the second diagram, it is the ideal index constellation of the left triangle, which allows application of formula (13.64). The last diagram can be solved easily via Eqs. (13.56) and (13.57).

13.5.4 Transformation of Indices

In general, Eq. (13.71) solves the integral if three elements (lines, vertices or triangles) are one step from an ideal index constellation [9, 3]. For example, if three lines have the index 1, or two triangles have $D/2+1$ and one vertex has $D-1$. Otherwise relation (13.71) is used to manipulate indices in order to reach an ideal index constellation. Simple lines with an index $a = 1$ in momentum space and $\alpha = D/2-1 = 1-\varepsilon/2$ in $\mathbf{x}$-space do not produce ideal index constellations. These properties are summarized in the following table:

	ideal	one step from ideal	simple lines
line	0	1	$1-\varepsilon/2$
vertex	$4-\varepsilon$	$3-\varepsilon$	$3-3\,\varepsilon/2$
triangle	$2-\varepsilon/2$	$3-\varepsilon/2$	$3-3\,\varepsilon/2$

.

An index transformation of order ε is required to reach an ideal index constellation. Apart from Eq. (13.71) the index constellation can also be changed by an insertion of a ϕ^2-vertex using Eq. (13.57), which changes a line into two lines with modified indices, generating an ideal index constellation in the adjacent vertex. Another option is the inversion of the integration variables, $x_\mu \longrightarrow x_\mu/x^2$. Finally, we can use the dual diagram with its transformed indices instead of the original integral.

13.5.5 Construction of Tables

The above rules (13.56), (13.57), (13.64) and (13.71) can be used to calculate the KITE-type and the BEQ- or BUG-type diagram for certain index constellations as in Eq. (13.73). For example, the application of the star-triangle relation reduces the KITE-type to a primitive diagram if a vertex or a triangle has an ideal index constellation. With the results for several index constellations, functional equations for the ε-expansion of the KITE-type or the BEQ-type integral depending on the line indices can be derived [3, 9]. The solutions of these equations are given in tables for indices of the form $1+a_i\varepsilon$. The KITE-type table was calculated by Kazakov up to ε^4. For the diagram

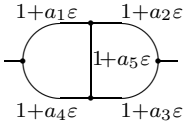

$$\equiv \frac{\mathrm{KI}\,(1+a_1\varepsilon,\ldots,1+a_5\varepsilon)}{(\mathbf{x}^2)^{5+\sum_i a_i\varepsilon-D}}\,, \tag{13.74}$$

the expansion has the following form:

$$\begin{aligned}\mathrm{KI}\,(1+a_1\varepsilon,\ldots,1+a_5\varepsilon) \;=\; \frac{1}{1-\varepsilon}\Big[\; & A_0\zeta(3)+\frac{A_1\zeta(4)}{2}\varepsilon+\frac{A_2\zeta(5)}{4}\varepsilon^2+\frac{A_3\zeta(6)}{8}\varepsilon^3 \\ & +\frac{A_4\zeta^2(3)}{8}\varepsilon^3-\frac{A_5\zeta(7)}{16}\varepsilon^4+\frac{A_6\zeta(3)\zeta(4)}{16}\varepsilon^4+\mathcal{O}(\varepsilon^5)\Big],\end{aligned} \tag{13.75}$$

with coefficients A_i depending only on the indices $a_1,\ldots,a_5$ and the combination $a^n=a_1^n+a_2^n+a_3^n+a_4^n$:

$$\begin{aligned}
A_0 \;&=\; 6,\quad A_1 \;=\; 9,\\
A_2 \;&=\; 42+30a+45a_5+10a^2+15a_5^2+15a_5a+10(a_1a_2+a_3a_4+a_1a_4+a_2a_3)+5(a_1a_3+a_2a_4),\\
A_3 \;&=\; \frac{5}{2}(A_2-6),\\
A_4 \;&=\; 46+42a+45a_5+14a^2+15a_5^2+33a_5a+50(a_1a_2+a_3a_4)+31(a_1a_3+a_2a_4)\\
&\quad +14(a_1a_4+a_2a_3)+6a_5a^2+6a_5^2a+24a_5(a_1a_2+a_3a_4)+12a_5(a_1a_3+a_2a_4)\\
&\quad +12(a_1a_2a_3+a_1a_2a_4+a_1a_3a_4+a_2a_3a_4)+12(a_1^2a_2+a_2^2a_1+a_3^2a_4+a_4^2a_3)\\
&\quad +6(a_1^2a_3+a_3^2a_1+a_2^2a_4+a_4^2a_2),\\
A_5 \;&=\; 294+402a+\frac{2223}{4}a_5+260a^2+\frac{3183}{8}a_5^2+516a_5a+386(a_1a_2+a_3a_4+a_1a_4+a_2a_3)\\
&\quad +\frac{575}{2}(a_1a_3+a_2a_4)+84a^3+\frac{567}{4}a_5^3\\
&\quad +168(a_1^2a_2+a_2^2a_1+a_3^2a_4+a_4^2a_3+a_4^2a_1+a_1^2a_4+a_2^2a_3+a_3^2a_2)\\
&\quad +\frac{441}{4}(a_1^2a_3+a_3^2a_2+a_2^2a_4+a_4^2a_2)+\frac{945}{4}a_5a^2+252a_5^2a+\frac{693}{2}a_5(a_1a_2+a_3a_4+a_1a_4+a_2a_3)\\
&\quad +\frac{945}{4}(a_1a_3+a_2a_4)a_5+210(a_1a_2a_3+a_1a_2a_4+a_1a_3a_4+a_2a_3a_4)+14a^4+\frac{189}{8}a_5^4\\
&\quad +42a_5a^3+\frac{189}{4}a_5^3a+\frac{525}{8}a_5^2a^2+\frac{357}{4}a_5^2(a_1a_2+a_3a_4+a_1a_4+a_2a_3)+\frac{105}{2}a_5^2(a_1a_3+a_2a_4)\\
&\quad +84a_5(a_1^2a_2+a_2^2a_1+a_3^2a_4+a_4^2a_3+a_1^2a_4+a_4^2a_1+a_2^2a_3+a_3^2a_2)\\
&\quad +\frac{189}{4}a_5(a_1^2a_3+a_3^2a_1+a_2^2a_4+a_4^2a_2)+\frac{357}{4}a_5(a_1a_2a_3+a_1a_3a_4+a_1a_2a_4+a_2a_3a_4)\\
&\quad +28(a_1^3a_2+a_2^3a_1+a_3^3a_4+a_4^3a_3+a_1^3a_4+a_4^3a_1+a_2^3a_3+a_3^3a_2)
\end{aligned}$$

$$
\begin{aligned}
&+14(a_1^3a_3+a_3^3a_1+a_2^3a_4+a_4^3a_2)+42(a_1^2a_2^2+a_3^2a_4^2+a_1^2a_4^2+a_2^2a_3^2)+\frac{189}{8}(a_1^2a_3^2+a_2^2a_4^2)\\
&+42(a_1^2a_2a_3+a_1^2a_2a_4+a_1^2a_3a_4+a_2^2a_1a_4+a_2^2a_1a_3+a_2^2a_3a_4\\
&\quad+a_3^2a_1a_4+a_3^2a_2a_4+a_3^2a_1a_2+a_4^2a_2a_3+a_4^2a_1a_3+a_4^2a_1a_2)+\frac{315}{4}a_1a_2a_3a_4,\\
A_6 \;&=\; 3(A_4-1),
\end{aligned}
\tag{13.76}
$$

This two-loop result can be used for **x**-space and for momentum space integrals since the KITE-type integral is dual to itself. Kazakov also calculated the the tables for the BEQ- and the BUG-type integrals with line indices of the form $\alpha_i = 1 + a_i\varepsilon$ up to order ε^2. Since these two are dual to each other, the **x**-space table for the BEQ-type integral has to be used for the momentum space integral of the BUG type and vice versa. For an integral of the BEQ type with the following form of the indices:

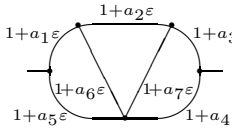

$$
\equiv\ \frac{\mathrm{BEQ}\,(1+a_1\varepsilon,\ldots,1+a_7\varepsilon)}{(\mathbf{x}^2)^{7+\sum_i a_i\varepsilon-3D/2}}\,,
\tag{13.77}
$$

the **x**-space BEQ-table up to ε^2 is given by [3, 9]

$$
\begin{aligned}
\mathrm{BEQ}(1+a_1\varepsilon,\ldots,1+a_7\varepsilon) \;&=\; \frac{1}{1-\varepsilon}\left[A_0\zeta(5)+\frac{A_1\zeta(6)}{2}\,\varepsilon+\frac{A_2\zeta^2(3)}{2}\,\varepsilon\right.\\
&\qquad\left.+\frac{A_3\zeta(7)}{4}\,\varepsilon^2+\frac{A_4\zeta(3)\zeta(4)}{4}\,\varepsilon^2+\mathcal{O}(\varepsilon^3)\right],
\end{aligned}
\tag{13.78}
$$

with the coefficients:

$$
\begin{aligned}
A_0 \;&=\; 20,\quad A_1 \;=\; 50,\quad A_2 \;=\; 20+6(a_4+a_5+a_6+a_7),\\
A_3 \;&=\; 7\left[\frac{380}{7}+20(a_1+a_3)+32a_2+17(a_4+a_5)+33(a_6+a_7)\right.\\
&\qquad+6(a_1^2+a_3^2)+8a_2^2+4(a_4^2+a_5^2)+8(a_6^2+a_7^2)+8(a_1+a_3)a_2+2(a_1a_4+a_3a_5)\\
&\qquad+6(a_1a_5+a_3a_4)+10(a_1a_6+a_3a_7)+6(a_1a_7+a_3a_6)+4a_1a_2+4(a_4+a_5)a_2\\
&\qquad+12(a_6+a_7)a_2+2a_4a_5+4(a_4a_6+a_5a_7)+6(a_4a_7+a_5a_6)+10a_6a_7\\
&\qquad\left.+\frac{1}{4}(a_4+a_5+a_6+a_7)+\frac{1}{8}(a_4+a_5+a_6+a_7)^2\right],\\
A_4 \;&=\; 3\left[20+6(a_4+a_5+a_6+a_7)\right].
\end{aligned}
\tag{13.79}
$$

The reduction algorithms of partial integration in momentum space solves the BEQ- and the BUG-diagram only if their line indices are integer. If they are not integer, these algorithms can be used to bring the two types to the standard form given by the tables. The diagrams determined by the tables are displayed in Fig. 13.9.

The tables enable us to calculate the N-type diagram with No. 4 in Fig. 13.2, which is the only one that requires the expansion of the BEQ-type diagram up to $\mathcal{O}(\varepsilon^2)$. The calculation is sketched in the next section.

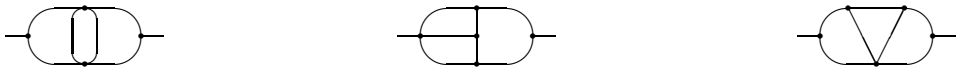

KITE type BUG type BEQ type

FIGURE 13.9 Types of diagrams given by the tables for indices of the form $a_i = 1 + a_i\varepsilon$.

13.6 Special Treatment of Generic Four- and Five-Loop Diagrams

There are only six diagrams where IR-rearrangement does not help avoiding the appearance of generic four- and five-loop diagrams and the NO type of Fig. 13.1. They are shown in Fig. 13.10. Even the combined use of the reduction algorithms and the tables is not sufficient to calculate

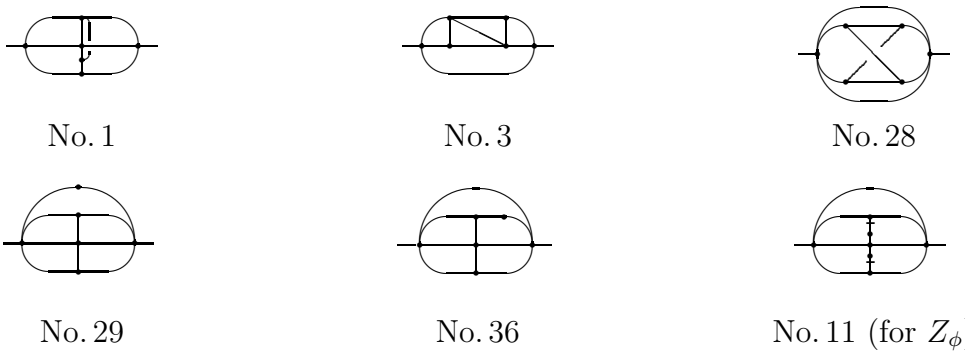

FIGURE 13.10 Diagrams whose calculation requires special methods.

them analytically. They need a special treatment. Three of the diagrams, Nos. 29, 36, and 11, are done in momentum space. The diagrams Nos. 29 and 36 are calculated by a clever application of the R-operation and momentum differentiation [1]. The diagram with vector indices emerging from differentiation of the quadratically divergent diagram No. 11 is solved by applying $\partial^2/\partial k_\mu \partial k_\mu$ to the integrals. The result is obtained by repeated partial integration.

Nos. 1, 3, and 28 have been solved in configuration space, they were first calculated numerically by GPXT. Analytical results up to $\mathcal{O}(\varepsilon^0)$ were found by Kazakov [9], applying the method of ideal index calculation of Section 13.5. The calculation of the N-shaped diagram is shown as an example.

13.6.1 N-Shaped Diagram

The N-shaped four-loop subdiagram has to be calculated up to $\mathcal{O}(\varepsilon^0)$. Being overall convergent without any subdivergences the constant term is the only one needed. The ε-expansion coefficients of the line indices of the subdiagram can thus be chosen arbitrarily. Relation (13.71) applied to the lower left vertex gives for the following index constellation:

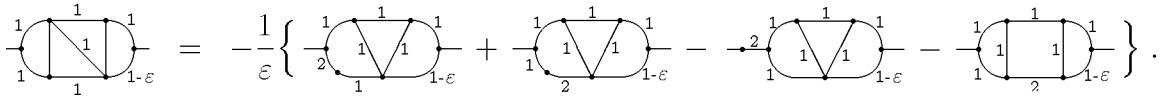

The chains can be integrated. The right vertex of the last diagram has an ideal index constellation, such that we obtain using (13.64):

$$
-\frac{1}{\varepsilon}\Bigg\{
\begin{aligned}
&2\,\nu(1)\,\nu(2)\,\nu(1-\varepsilon) && \\
&-\nu(2)\,\nu(1+\frac{1}{2}\varepsilon)\,\nu(1-\frac{3}{2}\varepsilon) && \\
&-\nu(1)\,\nu(2)\,\nu(1-\varepsilon) &&
\end{aligned}
\Bigg\}\,.
$$

The BEQ-type diagram is required up to $\mathcal{O}(\varepsilon^2)$ and can be deduced from Kazakov's expansions (13.75)–(13.79), yielding in $\mathbf{x}$-space:

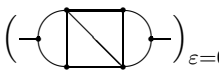

$$= \frac{1}{(\mathbf{x}^2)^{1-5\varepsilon/2}} \frac{441}{8} \zeta(7) \tag{13.80}$$

$$\xrightarrow{\text{FT}} \underbrace{\frac{\Gamma(1+2\varepsilon)}{\Gamma(1-5/2\varepsilon)}}_{=1+\mathcal{O}(\varepsilon)} \frac{1}{(\mathbf{k}^2)^{1+2\varepsilon}} \frac{441}{8} \zeta(7)\,, \tag{13.81}$$

where FT indicates a Fourier transformation. The required pole term of diagram No. 3 is then:

$\mathcal{K}\Big[$ 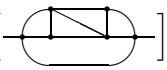 $\Big] = \mathcal{K}\Big[\frac{441}{8} \zeta(7) \underbrace{L(1+2\varepsilon,1)}_{=2/5\varepsilon+\mathcal{O}(\varepsilon^0)} \Big] = \frac{441}{20} \zeta(7)\, \varepsilon^{-1}\,.$ (13.82)

13.7 Computer-Algebraic Program

The momentum space algorithms of Section 13.4.3 together with the tables for the KITE-type integrals up to ε^4, for the BEQ- and the BUG-type up to ε^2, and the expansion of the loop function $L(a,b)$ up to ε^7 are implemented as a REDUCE program. It is based on the program LOOPS [7] that allows the calculation of primitive two-loop integrals with arbitrary line indices and free vector indices as well as the KITE-type integral with integer line indices without free vector indices. For the five-loop calculation, the expansion of the loop function $L(a,b)$ had to be extended up to $\mathcal{O}(\varepsilon^7)$ to account for extra poles arising in intermediate expressions. The program also contains the formulas in Section 13.4.3 and the tables in Section 13.5.5. The following types of diagrams can then be calculated:

1. Planar generic three-loop diagrams with integer line indices up to $\mathcal{O}(\varepsilon^3)$;

2. BEQ- and BUG-type integrals with $a_i = 1 + m_i\varepsilon/2$ up to $\mathcal{O}(\varepsilon^2)$;

3. KITE-type integrals

   - with arbitrary noninteger indices on the lines 1 and 4 *or* 2 and three up to $\mathcal{O}(\varepsilon^{7-L})$;
   - with arbitrary noninteger index on line 5 up to $\mathcal{O}(\varepsilon^4)$;
   - with indices of the form $a_i = 1 + m_i\varepsilon/2$ on all lines up to $\mathcal{O}(\varepsilon^4)$;

4. Primitive diagrams with L loops up to the order $\mathcal{O}(\varepsilon^{7-L})$.

All but six propagator-type integrals of the ϕ^4-theory up to five loops can be calculated with this program, as they can be reduced by IR-rearrangement and R^*-operation to one of the types above. The results for the 6 diagrams of Fig. 13.10 are inserted by hand.

We now proceed to sort all five-loop diagrams of the ϕ^4-theory according to the above types. The subdivisions depend on the IR-rearrangement and are somewhat arbitrary. There are 124 logarithmically divergent propagator-type integrals for $Z_g(g,\varepsilon^{-1})$ or $Z_{m^2}(g,\varepsilon^{-1})$ and 11 quadratically divergent ones for $Z_{m^2}(g,\varepsilon^{-1})$.

The 124 Logarithmically Divergent Integrals

They consist of (numbering corresponds to that in Appendix A):

a) 27 diagrams with cutvertices not contributing to the renormalization constants, with $\mathcal{K}\bar{R}G = \mathcal{K}\bar{R}G_1 \cdot \mathcal{K}\bar{R}G_2 = \sum_{i=1}^{L_1} C_i^1 \varepsilon^{-i} \sum_{i=1}^{5-L_1} C_i^2 \varepsilon^{-i} = \sum_{i=2}^{5} C_i' \varepsilon^{-i}$;

b) Insertions into simple loops. the inserted diagrams contain

- Generic four-loop diagrams (Nos. 3, 29, 36);
- Generic three-loop diagrams with integer indices (Nos. 24, 25, 26, 28, 34, 37, 53, 75, 111) or with noninteger indices (No. 27);
- Generic two-loop diagrams (KITE type) with the index a_5 noninteger (Nos. 32, 40, 42, 47, 58, 65, 73, 93, 98, 109, 112, 116, 123) or with index $a_1, \ldots, a_4$ noninteger (Nos. 38, 39, 44, 48, 51, 55, 59, 64, 67, 69, 74, 101);
- KITE-type integral with integer indices and primitive diagrams.

c) Insertions in KITE-type diagrams with index a_5 noninteger (Nos. 19, 79) or with index $a_1, \ldots, a_4$ noninteger (No. 57);

d) Generic five-loop diagrams (No. 1) and inserted results of diagrams (Nos. 3, 28, 29, 36).

For 26 diagrams the R^*-operation has to be carried out (Nos. 21, 32, 36, 37, 47, 53, 58, 61, 62, 65, 67, 73, 75, 79, 88, 91, 92, 93, 95, 101, 103, 105, 107, 109, 111, 116).

The 11 Quadratically Divergent p-Integrals

They consist of

a) 5 primitive diagrams (Nos. 1, 2, 3, 4, 5);

b) 6 diagrams require differentiation with respect to external momentum and infrared rearrangement

- 2 give known logarithmically divergent propagator-type integrals (Nos. 7, 8);
- 4 give integrals with free vector indices, 3 consisting of primitive or KITE-type integrals (Nos. 6, 9, 10) and 1 of a generic four-loop diagram (No. 11).

Appendix 13A Fourier Transformation of Simple Powers in D Dimensions

The Fourier transform of a simple power of $\mathbf{x}^2$ is again a simple power:

$$\frac{1}{(\mathbf{p}^2)^a} = \frac{\Gamma(D/2-a)}{\pi^{D/2}\Gamma(a)4^a} \int d^D x \, \frac{e^{i\mathbf{p}\cdot\mathbf{x}}}{(\mathbf{x}^2)^{D/2-a}} \, . \tag{13A.1}$$

We first split the $\mathbf{x}$-space into a component parallel to $\mathbf{p}$ and a $D-1$-dimensional space perpendicular to it:

$$\int d^D x \, \frac{e^{i\mathbf{p}\cdot\mathbf{x}}}{(\mathbf{x}^2)^{D/2-a}} = \int_{-\infty}^{\infty} dx_0 \cos(|\mathbf{p}|\, x_0) \int d^{D-1} x \frac{1}{(x_0^2+\mathbf{x}^2)^{D/2-a}}. \tag{13A.2}$$

The integration over the $D-1$-dimensional space can be carried out, and the right-hand side becomes

$$2\pi^{(D-1)/2}\,\frac{\Gamma(1/2-a)}{\Gamma(D/2-a)}\int_0^\infty dx_0 \frac{\cos(|\mathbf{p}|\,x_0)}{x_0^{1-2a}}. \tag{13A.3}$$

With the help of the integral formula

$$\int_0^\infty dy\,\frac{\cos(|\mathbf{p}|\,y)}{y^{1-2a}} = \frac{\pi}{2}\frac{|\mathbf{p}|^{-2a}}{\Gamma(1-2a)\,\cos(\frac{1-2a}{2}\pi)}, \tag{13A.4}$$

we find

$$\int d^Dx\,\frac{e^{i\mathbf{p}\cdot\mathbf{x}}}{(\mathbf{x}^2)^{D/2-a}} = \frac{\pi^{(D+1)/2}\,\Gamma(1/2-a)}{\Gamma(D/2-a)\,\Gamma(1-2a)\,\cos(\frac{1-2a}{2}\pi)}\,\frac{1}{(p^2)^a}\,, \tag{13A.5}$$

which can be trivially rewritten as

$$\frac{\pi^{D/2}\,\Gamma(a)4^a}{\Gamma(D/2-a)}\,\frac{\sqrt{\pi}\,\Gamma(1/2-a)}{4^a\Gamma(a)\,\Gamma(1-2a)\,\cos(\frac{1-2a}{2}\pi)}\,\frac{1}{(p^2)^a}\,. \tag{13A.6}$$

Using further

$$\cos(\pi/2-a\pi)=\sin(a\pi), \qquad \Gamma(1/2)=\sqrt{\pi}\,, \tag{13A.7}$$

and

$$\Gamma(1-2a)=\frac{\Gamma(1/2-a)\Gamma(1-a)}{\Gamma(1/2)}2^{-2a}\,, \tag{13A.8}$$

the right-hand side of (13A.6) can be brought to the form

$$\frac{\pi^{D/2}\Gamma(a)4^a}{\Gamma(D/2-a)}\,\underbrace{\frac{\pi}{\Gamma(a)\,\Gamma(1-a)\,\sin(a\pi)}}_{=1}\,\frac{1}{p^{2a}}, \tag{13A.9}$$

so that we finally obtain

$$\int d^Dx\,\frac{e^{i\mathbf{p}\cdot\mathbf{x}}}{(\mathbf{x}^2)^{D/2-a}} = 4^a\pi^{D/2}\frac{\Gamma(a)}{\Gamma(D/2-a)}\,\frac{1}{p^{2a}}\,. \tag{13A.10}$$

Appendix 13B Further Expansions of Gamma Function

In Appendix 8D, the Gamma function is expressed in terms of ψ functions. Here we supplement the formula by another expansion involving Riemann's ζ-functions. For this we recall the well-known expansion of the logarithm of the Gamma function:

$$\ln\Gamma(1+z) = -\gamma z + \sum_{m=2}^{\infty}(-1)^m\,\zeta(m)\,\frac{z^m}{m}, \tag{13B.1}$$

where γ is the *Euler constant*

$$\gamma = -\psi(1) = \sum_{m=2}^{\infty}(-1)^m\,\frac{\zeta(m)}{m} = 0.5772...\,, \tag{13B.2}$$

and $\zeta(x)$ is *Riemann's ζ function*:

$$\zeta(x) = \sum_{k=1}^{\infty}\frac{1}{k^x}\,. \tag{13B.3}$$

This representation can be generalized using the identity of the Gamma function $\Gamma(1+z) = z\Gamma(z)$, and the expansion $\ln(1+z) = \sum_{n=1}^{\infty}(-1)^{n+1}z^n/n$:

$$\begin{aligned}\ln\Gamma(2+z) &= \ln(1+z) + \ln\Gamma(1+z) \\ &= -\sum_{m=1}^{\infty}(-1)^m\frac{z^m}{m} - \gamma z + \sum_{m=2}^{\infty}(-1)^m\frac{z^m}{m}\zeta(m) \\ &= z(1-\gamma) + \sum_{m=2}^{\infty}(-1)^m\frac{z^m}{m}[\zeta(m)-1], \end{aligned} \tag{13B.4}$$

$$\begin{aligned}\ln\Gamma(3+z) &= \ln 2 + \ln(1+z/2) + \ln\Gamma(2+z) \\ &= \ln 2 - \sum_{m=1}^{\infty}(-1)^m\frac{(z/2)^m}{m} + z(1-\gamma) + \sum_{m=2}^{\infty}(-1)^m\frac{z^m}{m}[\zeta(m)-1] \\ &= \ln 2 + z\left(1+\frac{1}{2}-\gamma\right) + \sum_{m=2}^{\infty}(-1)^m\frac{z^m}{m}\left[\zeta(m)-1-\frac{1}{2^m}\right]. \end{aligned} \tag{13B.5}$$

In general one has

$$\ln\Gamma(n+z) = \ln[(n-1)!] + z\left[\sum_{k=1}^{n-1}\frac{1}{k} - \gamma\right] + \sum_{m=2}^{\infty}(-1)^m\frac{z^m}{m}\left[\zeta(m) - \sum_{k=1}^{n-1}\frac{1}{k^m}\right]. \tag{13B.6}$$

Inserting here the truncated zeta functions (13.17) with the property $\zeta^{(1)}(x) \equiv 0$ [see (13.18)] , this can be written as:

$$\Gamma(n+z) = (n-1)!\,\exp\left\{-z\left[\gamma - \zeta^{(n)}(1)\right] + \sum_{m=2}^{\infty}(-1)^m\frac{z^m}{m}\left[\zeta(m) - \zeta^{(n)}(m)\right]\right\}. \tag{13B.7}$$

Note that this is the manifestly finite version of the more symmetric but not well-defined expression:

$$\Gamma(n+z) \stackrel{n\geq 0}{=} n!\,\exp\left\{\sum_{m=1}^{\infty}(-1)^m\frac{z^m}{m}\left[\zeta(m) - \zeta^{(n)}(m)\right]\right\}, \tag{13B.8}$$

where γ has been set equal to $\zeta(1)$. In fact, the quantity $\zeta(1)$ is divergent, since the truncated sum $\zeta^{(n)}(1)$ grows with n like $\log n + \gamma$.

In Appendix 8D we gave an expansion of the Gamma function near integer arguments in terms of the Digamma functions [see Eq. (8D.23)]:

$$\Gamma(n+1+\varepsilon) = n!\left\{1 + \varepsilon\,\psi(n+1) + \frac{\varepsilon^2}{2}\left[\psi'(n+1) + \psi(n+1)^2\right] + O(\varepsilon^3)\right\}. \tag{13B.9}$$

To see the equivalence of the two expansions, we use the truncated zeta function (13.17) to rewrite (8D.12) and (8D.13) as

$$\psi(n+1) = \zeta^{(n+1)}(1) - \gamma, \tag{13B.10}$$

$$\psi'(n+1) = -\zeta^{(n+1)}(2) + \frac{\pi^2}{6} = -\zeta^{(n+1)}(2) + \zeta(2). \tag{13B.11}$$

Inserting this into (13B.9), we obtain

$$\begin{aligned}\Gamma(n+\varepsilon+1) = n!\Bigg(&1 + \varepsilon\left\{\zeta^{(n+1)}(1) - \gamma\right\} \\ &+ \frac{\varepsilon^2}{2}\left\{-\zeta^{(n+1)}(2) + \zeta(2) + [\zeta^{(n+1)}(1) - \gamma]^2\right\} + \mathcal{O}(\varepsilon^3)\Bigg), \end{aligned} \tag{13B.12}$$

which is the ε-expansion of Eq. (13B.8) up to second order in ε.

Notes and References

The citations in the text refer to:

[1] K.G. Chetyrkin, F.V. Tkachov, Nucl. Phys. B **192**, 159 (1981).

[2] K.G. Chetyrkin, A.L. Kataev, and F.V. Tkachov, Nucl. Phys. B **174**, 345 (1980).

[3] D.I. Kazakov, Phys. Lett. B **133**, 406 (1983); Theor. Math. Phys. **61**, 84 (1985).
The author used the term 'method of uniqueness', but 'method of ideal index constellations' is more descriptive.

[4] S.G. Gorishny, S.A. Larin, L.R. Surguladze, and F.V. Tkachov, Comp. Phys. Comm. **55**, 381, (1989).

[5] See Ref. [2] and [4]. The original name used by those authors was *G-scheme* since the authors denote the loop integrals L by G. The name L-scheme is an adaptation of their name to our notation.

[6] Some authors refer to this as the $\overline{\text{MS}}$-scheme, which is different from ours defined in Eq. (13.24).

[7] For this purpose we extended an available program LOOPS written by
L.R. Surguladze and F.V. Tkachov, Comp. Phys. Comm. **55**, 205 (1989),
which gave the expansion terms only up to $\mathcal{O}(\varepsilon^4)$.

[8] This is the redefinition of g or μ used in the program LOOPS of Ref. [7].

[9] D.I. Kazakov, Theor. Math. Phys. **58**, 223 (1984).